SUPPLEMENTARY INFORMATION (SI)

Enhancing Indacenodithiophene Acceptor Crystallinity via Substituent Manipulation Increases Organic Solar Cell Efficiency

Thomas J. Aldrich,[†] Steven M. Swick,[†] Ferdinand S. Melkonyan,*[,†,‡] Tobin J. Marks*[,†,‡]

[†] Department of Chemistry and the Materials Research Center, Northwestern University, 2145 Sheridan Road, Evanston, Illinois 60208, United States.

[‡] Department of Materials Science and Engineering and Argonne Northwestern Solar Energy Research Center (ANSER), Northwestern University, 2145 Sheridan Road, Evanston, Illinois 60208, United States.

* To whom correspondence should be addressed. E-mail: F. S. M. (f-melkonyan@northwestern.edu), T. J. M. (t-marks@northwestern.edu).

Table of Contents

1. Materials and Methods

All reagents were purchased from commercial sources and were used without further purification unless noted otherwise. **ITIC-C6** (**ITIC**, OSO004, lot no. YY11135) and **PBDB-T** (OSO804, lot no. YY11208) were purchased from 1-Materials. $Pd(PPh_3)_4$ was purchased from Strem Chemicals and stored in an argon-filled glovebox (< 0.5 ppm O_2). The polymerization solvent toluene was purchased from Sigma-Aldrich as anhydrous solvent, and was additionally vacuum-transferred from Na/K, degassed by freeze-pump-thaw methods, and stored in an argon-filled glovebox (< 0.5 ppm O_2).

Copolymer molecular weights were determined on a Polymer Laboratories PL-GPC 220 instrument equipped with a set of three PLgel 10 μm mixed-B columns using 1,2,4-trichlorobenzene (stabilized with 125 ppm of BHT) as eluent at 150 °C and calibrated to polystyrene standards. Copolymer samples were pre-dissolved at ~ 1.00 mg/mL concentration in 1,2,4-trichlorobenzene while shaking for 2 h at 150 °C.

NMR spectra were recorded on Agilent DD MR-400 (FT, 400 MHz, ^{1}H; 101 MHz, ^{13}C; 376 MHz, ^{19}F), Bruker Avance III (FT, DCH Cryoprobe, 500 MHz, ^{1}H; 126 MHz, ^{13}C) spectrometers at ambient temperature unless noted otherwise. High Temperature NMR spectra of copolymers were recorded at 120 °C on an Agilent DD2 (FT, 500 MHz, ^{1}H; 470 MHz, ^{19}F) spectrometer temperature-calibrated with ethylene glycol standards and copolymer samples were prepared at a concentration of 2.0 mg/mL in $C_2D_2Cl_4$. **ITIC-CX** NMR samples were prepared at a concentration of 2.0 mg/mL. Chemical shifts for ^{1}H and ^{13}C spectra are referenced to residual protio-solvent signals (δ ^{1}H = 7.26 for $CDCl_3$, 5.32 for CD_2Cl_2, 6.00 for $C_2D_2Cl_4$; δ ^{13}C = 77.16 for $CDCl_3$, 53.84 for CD_2Cl_2) and chemical shifts are reported in ppm.

Elemental Analysis was performed by Midwest Microlab. HRMS was performed on an Agilent 6210A LC-TOF instrument.

Photovoltaic data are reported as mean values with ± 1σ deviation. Statistical analysis was performed using Origin 2015 Pro statistics package.

2. Materials Synthesis and Purification

Scheme S1. Synthesis of **ITIC-C3.**

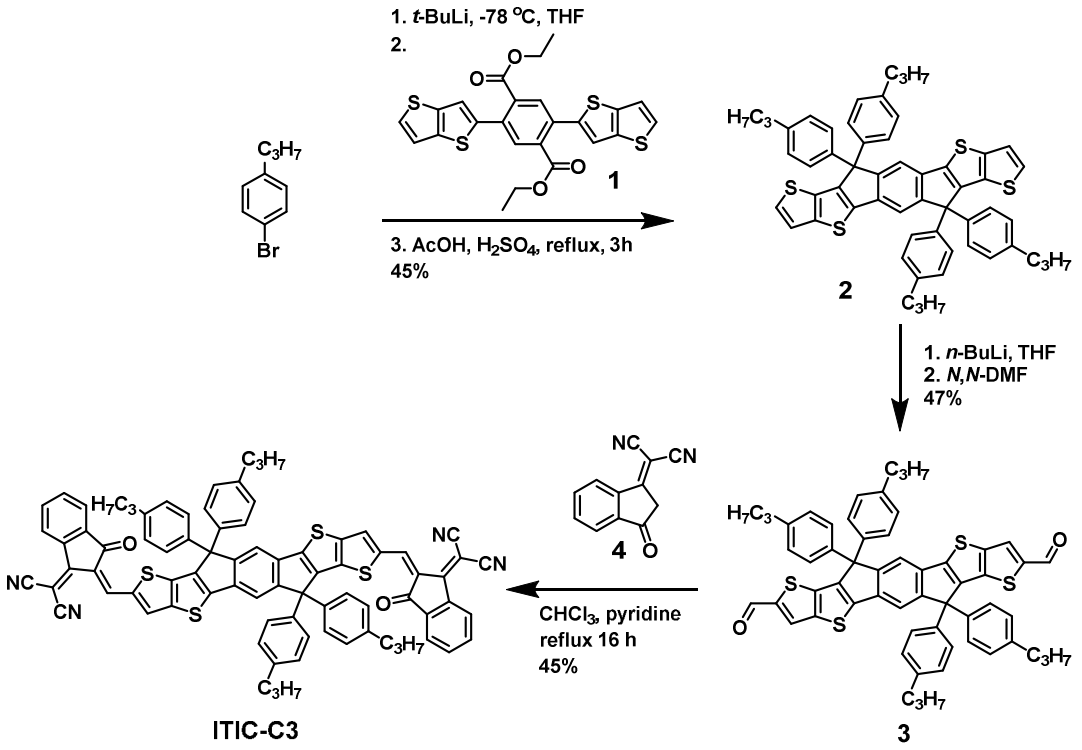

1: **1** was prepared following reported procedures[1] and purified by column chromatography (SiO_2: hexanes:DCM 50:50 → 0:100. The NMR spectroscopic data are in good agreement with those previously reported.

^{1}H NMR (400 MHz, CD_2Cl_2) δ 7.88 (s, 2H), 7.45 (d, J = 5.1 Hz, 2H), 7.34 – 7.27 (m, 4H), 4.24 (q, J = 7.1 Hz, 4H), 1.14 (t, J = 7.1 Hz, 6H).

2: In an oven-dried 100 mL Schlenk flask, **1-Bromo-4-propylbenzene** (1.99 g, 5.0 eq., 10.0 mmol) was dissolved in anhydrous THF (30 mL) under N_2-atmosphere and then cooled to –78 °C. *t*-BuLi [Caution! Pyrophoric!] (1.81 M in pentane, 11.1 mL, 10.0 eq., 20.0 mmol) was added dropwise and then stirred for 1 h at –78 °C. **1** (0.997 g, 1.0 eq., 2.0 mmol) was added in one portion and the solution was warmed to r.t. slowly overnight. The solution was poured into sat. NH_4Cl (250 mL) and extracted with EtOAc (3 × 100 mL). The organic layer was dried over

Na_2SO_4, filtered, and then concentrated under reduced pressure. The residue was added to a flask containing glacial acetic acid (100 mL) and concentrated H_2SO_4 (2 mL) and the resulting suspension was heated at reflux for 3 h. under N_2-atmosphere. The reaction mixture was cooled to r.t. and then poured into DCM (200 mL). The organic layer was washed with H_2O (2 × 200 mL), sat. K_2CO_3 (200 mL), and H_2O (2 × 200 mL). The organic layer was dried over Na_2SO_4, filtered, and then concentrated under reduced pressure. The residue was purified by column chromatography (SiO_2: hexanes:DCM 100:0 → 75:25) and then recrystallized from toluene (50 mL) at –78 °C. The product was dried under vacuum (<20 mTorr) at 60 °C for 12 h and obtained as a yellow solid (0.771 g, 0.91 mmol, 45%).

^{1}H NMR (500 MHz, CD_2Cl_2) δ 7.55 (s, 2H), 7.31 (s, 4H), 7.18 (d, J = 8.3 Hz, 8H), 7.10 (d, J = 8.2 Hz, 8H), 2.54 (t, J = 7.7 Hz, 8H), 1.76 – 1.54 (m, 8H), 0.93 (t, J = 7.3 Hz, 12H). ^{13}C NMR (126 MHz, CD_2Cl_2) δ 153.8, 146.5, 143.5, 142.4, 142.2, 140.6, 136.4, 133.9, 129.0, 128.3, 127.0, 120.9, 117.2, 63.4, 38.0, 24.9, 14.1. HRMS: Calcd for $[C_{56}H_{50}S_4 + H]^+$, m/z = 851.2868. Found: m/z = 851.2850 $[M+H]^+$.

3: In an oven-dried 50 mL Schlenk flask, **2** (426 mg, 1.0 eq., 0.50 mmol) was dissolved in anhydrous THF (20 mL) under N_2-atmosphere and then cooled to –78 °C. *n*-BuLi [Caution! Pyrophoric!] (2.71 M in hexanes, 0.46 mL, 2.5 eq., 1.25 mmol) was added dropwise and then stirred for 15 min. at –78 °C. The solution was removed from the cooling bath, allowed to warm to r.t. over the course of 1 h., and then cooled to –78 °C. *N*,*N*-DMF (116 µL, 110 mg, 3.0 eq., 1.5 mmol) was added dropwise and the solution was warmed to r.t. slowly overnight. The solution was poured into brine (100 mL) and extracted with $CHCl_3$ (3 × 50 mL). The organic layer was dried over Na_2SO_4, filtered, and then concentrated under reduced pressure. The residue was purified by column chromatography (SiO_2: hexanes:DCM 70:30 → 20:80). The product was dissolved in DCM and then precipitated into hexanes (100 mL), cooled to –20 °C, and then filtered. The product was dried under vacuum (<20 mTorr) at 60 °C for 12 h and obtained as a goldenrod solid (214 mg, 0.236 mmol, 47%).

^{1}H NMR (500 MHz, CD_2Cl_2) δ 9.88 (s, 2H), 7.98 (s, 2H), 7.67 (s, 2H), 7.17 (d, J = 8.3 Hz, 8H), 7.12 (d, J = 8.3 Hz, 8H), 2.54 (t, J = 7.6 Hz, 8H), 1.67 – 1.55 (m, 8H), 0.93 (t, J = 7.3 Hz, 12H). ^{13}C NMR (126 MHz, CD_2Cl_2) δ 183.2, 155.1, 149.8, 147.0, 144.9, 142.6, 142.5, 140.0, 139.7,

136.8, 130.5, 129.2, 128.2, 118.4, 63.6, 38.0, 24.9, 14.1. HRMS: Calcd for $[C_{58}H_{50}O_2S_4 + H]^+$, m/z = 907.2766. Found: m/z = 907.2722 $[M+H]^+$.

4: **4** was prepared following reported procedures.[2] The NMR spectroscopic data are in good agreement with those previously reported.

^{1}H NMR (400 MHz, $CDCl_3$) δ 8.66 (d, *J* = 7.8 Hz, 1H), 7.99 (d, *J* = 7.8 Hz, 1H), 7.90 (td, *J* = 7.6, 1.4 Hz, 1H), 7.85 (td, *J* = 7.4, 0.9 Hz, 1H), 3.73 (s, 2H).

ITIC-C3: In an oven-dried 50 mL round bottom flask equipped with reflux condenser, **3** (90.7 mg, 1.0 eq., 0.10 mmol), and **4** (58.3 mg, 3.0 eq., 0.30 mmol) were dissolved in a mixture of anhydrous $CHCl_3$ (30 mL) and anhydrous pyridine (0.6 mL) under N_2-atmosphere. The reaction was heated to reflux for 16 h. The reaction mixture was cooled to r.t. and then dripped into vigorously stirring MeOH (300 mL) and stirred for 30 min. The precipitate was filtered and the residue was purified by column chromatography (SiO_2: DCM). The product was then precipitated into MeOH (100 mL), filtered, and dried under vacuum (<100 mTorr) at 60 °C for 24 h. The product was obtained as a dark solid (56.3 mg, 0.045 mmol, 45%).

^{1}H NMR (500 MHz, CD_2Cl_2) δ 8.85 (s, 2H), 8.67 (d, *J* = 7.6 Hz, 2H), 8.23 (s, 2H), 7.93 – 7.87 (m, 2H), 7.79 (td, *J* = 7.6, 1.4 Hz, 2H), 7.75 (t, *J* = 7.2 Hz, 2H), 7.72 (s, 2H), 7.24 (d, *J* = 8.3 Hz, 8H), 7.16 (d, *J* = 8.3 Hz, 8H), 2.56 (t, *J* = 7.6 Hz, 8H), 1.68 – 1.57 (m, 8H), 0.94 (t, *J* = 7.3 Hz, 12H). ^{13}C NMR (126 MHz, CD_2Cl_2) δ 188.4, 160.8, 156.0, 152.9, 147.9, 146.7, 144.1, 142.8, 140.5, 139.8, 139.4, 138.3, 137.3, 137.1, 135.6, 134.9, 129.3, 128.3, 125.6, 124.1, 123.6, 118.9, 115.1, 115.0, 70.1, 63.6, 38.0, 24.9, 14.2. HRMS: Calcd for $[C_{82}H_{58}N_4O_2S_4 + H]^+$, m/z = 1259.3515. Found: m/z = 1259.3495 $[M+H]^+$.

Scheme S2. Synthesis of **ITIC-C9**.

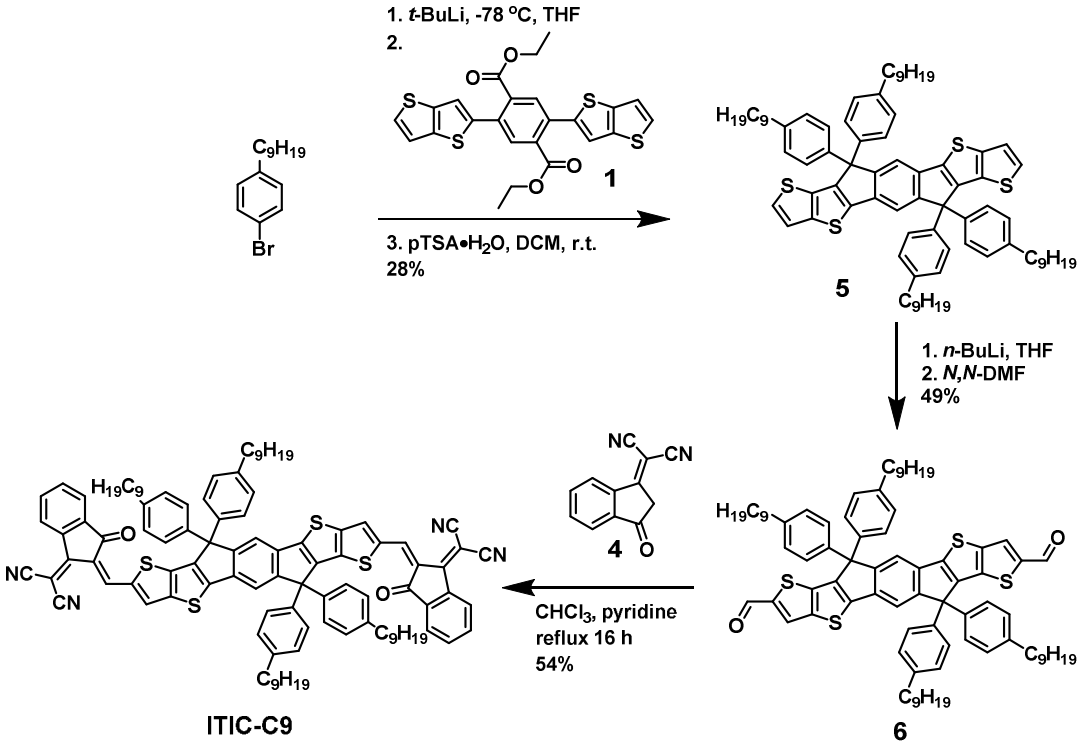

5: In an oven-dried 100 mL Schlenk flask, **1-Bromo-4-nonylbenzene** (2.83 g, 5.0 eq., 10.0 mmol) was dissolved in anhydrous THF (30 mL) under N_2-atmosphere and then cooled to –78 °C. *t*-BuLi [Caution! Pyrophoric!] (1.81 M in pentane, 11.1 mL, 10.0 eq., 20.0 mmol) was added dropwise and then stirred for 1 h at –78 °C. **1** (0.997 g, 1.0 eq., 2.0 mmol) was added in one portion and the solution was warmed to r.t. slowly overnight. The solution was poured into sat. NH_4Cl (250 mL) and extracted with EtOAc (3 × 100 mL). The organic layer was dried over Na_2SO_4, filtered, and then concentrated under reduced pressure. The residue was dissolved in DCM (30 mL) and then pTSA·H_2O (0.761 g, 2.0 eq., 4.0 mmol) was added in one portion. The solution was stirred for 3 h. at r.t. and then poured into H_2O (50 mL) and extracted with DCM (2 × 20 mL). The organic layer was dried over Na_2SO_4, filtered, and then concentrated under reduced pressure. The residue was purified by column chromatography (SiO_2: hexanes:DCM 100:0 → 90:10), then precipitated into MeOH (200 mL) and filtered. The product was dried under vacuum (<20 mTorr) at 60 °C for 12 h and obtained as a yellow solid (0.665 g, 0.56 mmol, 28%).

^{1}H NMR (500 MHz, CD_2Cl_2) δ 7.55 (s, 2H), 7.31 (s, 4H), 7.18 (d, *J* = 8.2 Hz, 8H), 7.10 (d, *J* = 8.2 Hz, 8H), 2.56 (t, *J* = 7.7 Hz, 8H), 1.67 – 1.54 (m, 8H), 1.43 – 1.11 (m, 48H), 0.87 (t, *J* = 6.9 Hz, 12H). ^{13}C NMR (126 MHz, CD_2Cl_2) δ 153.8, 146.5, 143.5, 142.5, 142.4, 140.5, 136.4, 133.9, 128.9, 128.3, 127.0, 120.9, 117.3, 63.4, 54.3, 54.1, 53.8, 53.6, 53.4, 35.9, 32.3, 31.9, 29.9, 29.9, 29.9, 29.7, 23.1, 14.3. HRMS: Calcd for $[C_{80}H_{98}S_4 + H]^+$, m/z = 1187.6624. Found: m/z = 1187.6617 $[M+H]^+$.

6: In an oven-dried 50 mL Schlenk flask, **5** (594 mg, 1.0 eq., 0.50 mmol) was dissolved in anhydrous THF (20 mL) under N_2-atmosphere and then cooled to –78 °C. *n*-BuLi [Caution! Pyrophoric!] (2.71 M in hexanes, 0.46 mL, 2.5 eq., 1.25 mmol) was added dropwise and then stirred for 15 min. at –78 °C. The solution was removed from the cooling bath, allowed to warm to r.t. over the course of 1 h., and then cooled to –78 °C. *N*,*N*-DMF (116 µL, 110 mg, 3.0 eq., 1.5 mmol) was added dropwise and the solution was warmed to r.t. slowly overnight. The solution was poured into brine (100 mL) and extracted with $CHCl_3$ (3 × 50 mL). The organic layer was dried over Na_2SO_4, filtered, and then concentrated under reduced pressure. The residue was purified by column chromatography (SiO_2: hexanes:DCM 85:15 → 55:45). The product was dissolved in DCM and then precipitated into MeOH (100 mL) and then filtered. The product was dried under vacuum (<20 mTorr) at 60 °C for 12 h and obtained as a goldenrod solid (303.8 mg, 0.244 mmol, 49%).

^{1}H NMR (500 MHz, CD_2Cl_2) δ 9.88 (s, 2H), 7.98 (s, 2H), 7.67 (s, 2H), 7.16 (d, *J* = 8.1 Hz, 8H), 7.11 (d, *J* = 8.3 Hz, 8H), 2.56 (t, *J* = 7.9 Hz, 8H), 1.69 – 1.54 (m, 8H), 1.36 – 1.18 (m, 48H), 0.86 (t, *J* = 6.7 Hz, 12H). ^{13}C NMR (126 MHz, CD_2Cl_2) δ 183.2, 155.1, 149.8, 147.0, 144.9, 142.9, 142.5, 140.1, 139.6, 136.8, 130.5, 129.1, 128.2, 118.4, 63.6, 35.9, 32.3, 31.8, 29.9, 29.9, 29.8, 29.7, 23.1, 14.3. HRMS: Calcd for $[C_{82}H_{98}O_2S_4 + H]^+$, m/z = 1243.6522. Found: m/z = 1243.6517 $[M+H]^+$.

ITIC-C9: In an oven-dried 50 mL round bottom flask equipped with reflux condenser, **6** (124.4 mg, 1.0 eq., 0.10 mmol), and **4** (58.3 mg, 3.0 eq., 0.30 mmol) were dissolved in a mixture of anhydrous $CHCl_3$ (30 mL) and anhydrous pyridine (0.6 mL) under N_2-atmosphere. The reaction was heated to reflux for 16 h. The reaction mixture was cooled to r.t. and then dripped into

vigorously stirring MeOH (300 mL) and stirred for 30 min. The precipitate was filtered and the residue was purified by column chromatography (SiO_2: $CHCl_3$). The product was then precipitated into MeOH (100 mL), filtered, and dried under vacuum (<100 mTorr) at 60 °C for 24 h. The product was obtained as a dark solid (85.8 mg, 0.054 mmol, 54%).

^{1}H NMR (500 MHz, CD_2Cl_2) δ 8.85 (s, 2H), 8.67 (d, *J* = 7.6 Hz, 2H), 8.22 (s, 2H), 7.95 – 7.86 (m, 2H), 7.79 (td, *J* = 7.6, 1.4 Hz, 2H), 7.77 – 7.73 (m, 2H), 7.71 (s, 2H), 7.23 (d, *J* = 8.3 Hz, 8H), 7.16 (d, *J* = 8.3 Hz, 8H), 2.57 (t, *J* = 7.7 Hz, 8H), 1.64 – 1.55 (m, 8H), 1.42 – 1.09 (m, 48H), 0.85 (t, *J* = 6.9 Hz, 12H). ^{13}C NMR (126 MHz, CD_2Cl_2) δ 188.4, 160.7, 156.0, 152.9, 147.9, 146.7, 144.1, 143.1, 140.5, 139.9, 139.4, 138.3, 137.3, 137.1, 135.6, 134.9, 129.2, 128.3, 125.6, 124.1, 123.6, 118.9, 115.1, 115.0, 70.1, 63.6, 35.9, 32.3, 31.8, 29.9, 29.9, 29.9, 29.7, 23.1, 14.3. HRMS: Calcd for $[C_{106}H_{106}N_4O_2S_4 + H]^+$, m/z = 1596.7305. Found: m/z = 1596.7309 $[M+H]^+$.

Scheme S3. Synthesis of **PBDB-TF**.

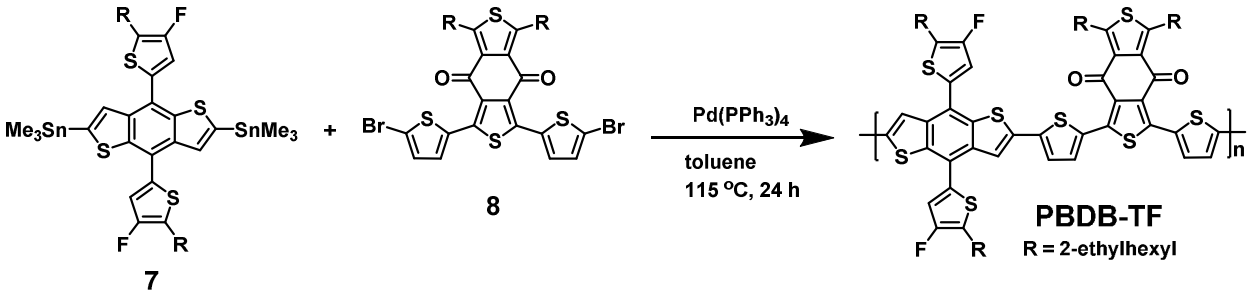

7: **7** was prepared following reported procedures.[3] The NMR spectroscopic data are in good agreement with those previously reported.

^{1}H NMR (400 MHz, CD_2Cl_2) δ 7.69 (s, 2H), 7.18 (s, 2H), 2.81 (d, J = 6.8 Hz, 4H), 1.68 (hept, J = 6.1 Hz, 2H), 1.49 – 1.25 (m, 16H), 1.03 – 0.85 (m, 12H), 0.42 (s, 18H). ^{19}F NMR (376 MHz, CD_2Cl_2) δ -133.82.

8: **8** was prepared following reported procedures.[4] The NMR spectroscopic data are in good agreement with those previously reported.

^{1}H NMR (400 MHz, CD_2Cl_2) δ 7.44 (d, J = 4.1 Hz, 2H), 7.08 (d, J = 4.1 Hz, 2H), 3.49 – 3.08 (m, 4H), 1.76 (hept, J = 6.2 Hz, 2H), 1.48 – 1.23 (m, 16H), 1.02 – 0.83 (m, 12H).

PBDB-TF: The **PBDB-TF** polymerization reaction was set up in an argon-filled glovebox (<0.5 ppm O_2). An oven-dried 5 mL Wheaton V-vial equipped with a stir bar was charged with: **7** (94.05 ± 0.03 mg, 1.00 eq., 0.100 mmol), **8** (76.67 ± 0.03 mg, 1.00 eq., 0.100 mmol), $Pd(PPh_3)_4$ (5.78 ± 0.03 mg, 5.0 mol%, 5.0×10^{-3} mmol), and toluene (3.33 ± 0.01 mL). The vial was sealed with a Mininert pressure screw cap and removed from the glovebox. The reaction mixture was heated and stirred at 110 °C for 24 h using a temperature-controlled stirring hotplate (preheated and equilibrated at 110 °C). Then, the reaction mixture was cooled to r.t. and 0.1 mL of 2-(tributylstannyl)thiophene was added through the Mininert valve. The reaction mixture was heated and stirred at 110 °C for an additional 2.0 h. Then, the reaction mixture was cooled to r.t. and 0.2 mL of 2-bromothiophene was added through the Mininert valve. The reaction mixture was heated and stirred at 110 °C for an additional 2.0 h. After cooling to r.t., the reaction mixture was dripped into MeOH (100 mL) while vigorously stirring. After 1 h., the polymer was transferred to a cellulose extraction thimble and subjected to Soxhlet extraction using methanol, acetone, hexanes, and chlorobenzene as solvents. After the final extraction with chlorobenzene,

the polymer solution was concentrated under reduced pressure, and then dripped into MeOH (100 mL) while vigorously stirring. The polymer product was collected by filtration and dried overnight under high vacuum (100 mTorr) at 60 °C to afford a dark solid. (118 mg, 97%, M_n = 17.9 kg/mol, $Đ$ = 2.73).

Anal. Calcd for $C_{68}H_{76}F_2O_2S_8$ (%): C, 66.96; H, 6.28. Found (%): C, 67.07; H, 6.33.

3. UV-vis Absorption Spectroscopy

The **ITIC-CX** solution and film UV-vis spectra were recorded on a Varian Cary 5000 UV-vis-NIR spectrophotometer. The **ITIC-CX** solutions were prepared at 0.0100 mg/mL in chlorobenzene and measured at ambient temperature. The **ITIC-CX** film optical absorption spectra were recorded from films cast from chlorobenzene (10.0 mg/mL, 2000 rpm) onto glass slides. The copolymer solution and film UV-vis spectra were recorded on a Varian Cary 100 UV-vis spectrophotometer. The copolymer solutions were prepared at 0.010 mg/mL in chlorobenzene and measured at ambient temperature. The copolymer film optical absorption spectra were recorded from films cast from chlorobenzene (5.0 mg/mL, 2500 rpm) onto glass slides.

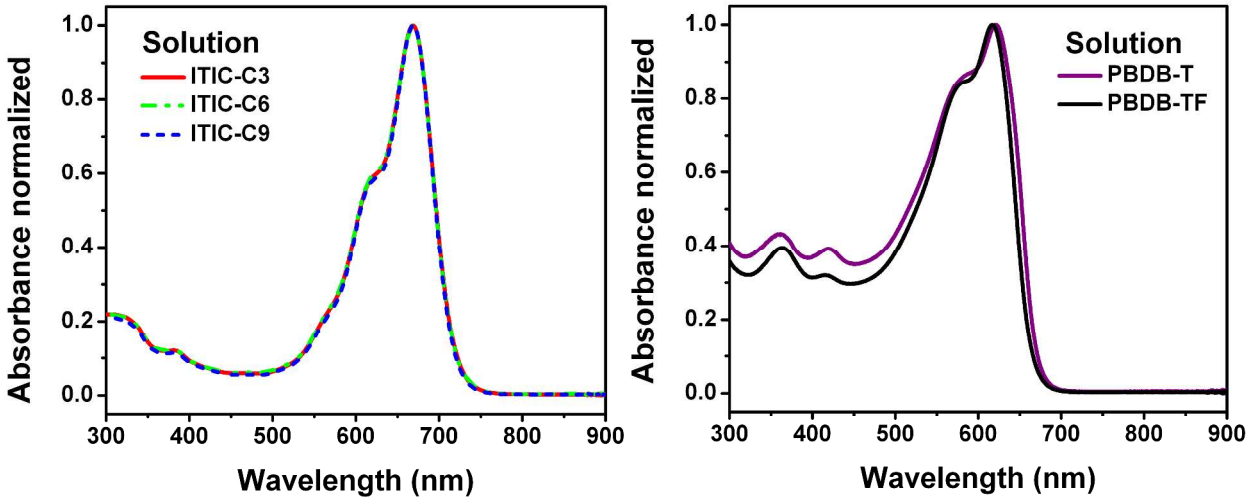

Figure S1. Solution UV-vis absorption spectra of **ITIC-CX** and donor polymers.

Table S1. Summary of the optical properties of the **ITIC-CX** acceptors and donor polymers.

Material	Solution λ_{max} (nm)	$\varepsilon \times 10^{-5}$ ($M^{-1}cm^{-1}$)‡	Film λ_{max} (nm)	Onset (nm)§	E_g^{opt} (eV)#
ITIC-C3	669	1.7	713	789	1.57
ITIC-C6	669	1.6	710	779	1.59
ITIC-C9	669	1.7	709	778	1.59
PBDB-T	621	-	625	674	1.84
PBDB-TF	617	-	621	670	1.85

‡ Extinction coefficient in solution (0.0100 mg/mL). § Absorption edge of thin film. # Optical energy gap estimated from the absorption edge of the thin film.

4. Cyclic Voltammetry (CV)

The electrochemical properties of the **ITIC-CX** acceptors and copolymers were investigated as thin films in deoxygenated anhydrous acetonitrile under nitrogen at a scan rate of 100 mV/s using 0.1 M tetrakis(n-butyl)ammonium hexafluorophosphate [$(n\text{-Bu})_4N^+PF_6^-$] as the supporting electrolyte. Pt electrodes were used as both the working and counter electrodes, and with Ag/Ag^+(sat. NaCl) as the pseudoreference electrode. **ITIC-CX** and copolymer films were drop-cast onto the Pt working electrode from a 5 mg/mL $CHCl_3$ solution. A ferrocene/ferrocenium (Fc/Fc^+) redox couple was used as internal standard and was assigned an absolute energy of –4.88 eV vs vacuum.[5] The HOMO energies of materials were determined according to the equation $E_{HOMO} = -(E_{ox}^{onset} + 4.88)$, where E_{ox}^{onset} is the onset of oxidation potential relative to the measured Fc/Fc^+ redox couple. The Fc/Fc^+ redox couple was found at 0.451 V relative to the Ag/Ag^+ electrode.

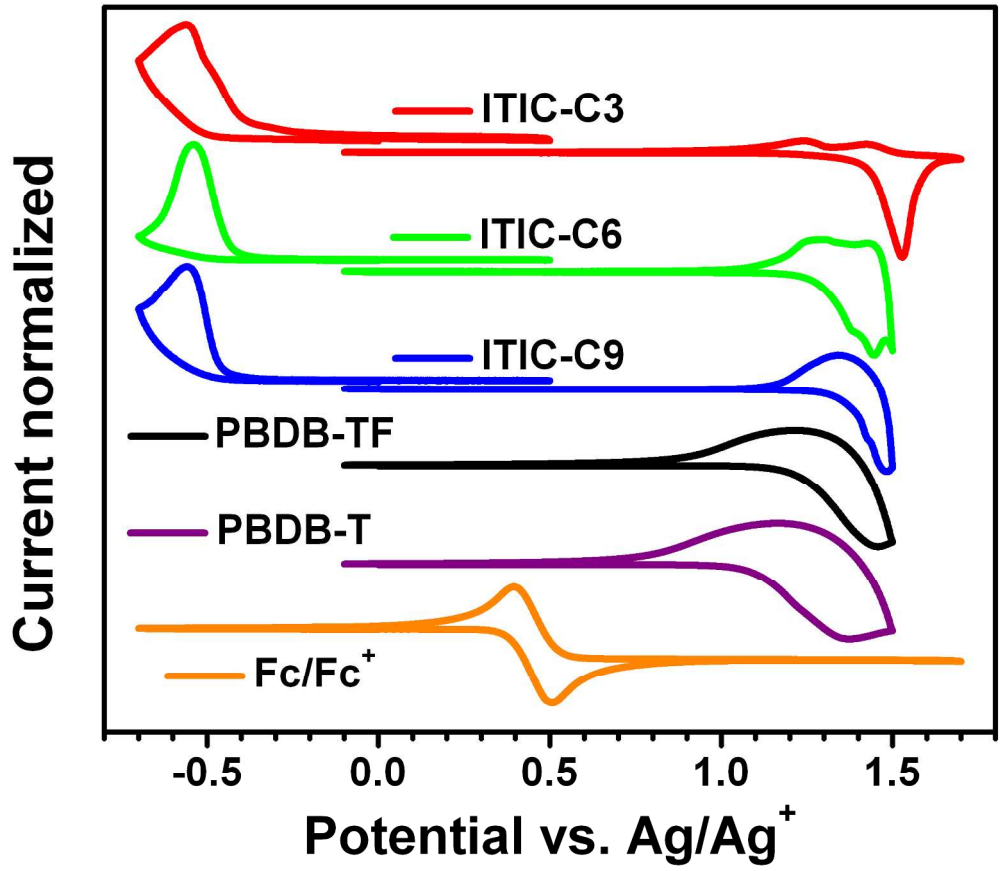

Figure S2. Cyclic voltammograms of the **ITIC-CX** and donor polymers.

Table S2. Summary of the electrochemical properties of the **ITIC-CX** and donor polymers.

Material	E_{ox}^{onset} vs. Fc/Fc$^+$ (eV)	E_{HOMO}[†] (eV)	E_{red}^{onset} vs. Fc/Fc$^+$ (eV)	E_{LUMO}[‡] (eV)
ITIC-C3	0.978	–5.86	–0.831	–4.05
ITIC-C6	0.824	–5.70	–0.884	–4.00
ITIC-C9	0.898	–5.78	–0.914	–3.97
PBDB-T	0.644	–5.52	-	–3.68[§]
PBDB-TF	0.777	–5.66	-	–3.81[§]

[†] Calculated according to: $E_{HOMO} = -(E_{ox}^{onset} + 4.88)$. [‡] Calculated according to $E_{LUMO} = -(E_{red}^{onset} + 4.88)$. [§] Calculated according to: $E_{LUMO} = E_g^{opt} + E_{HOMO}$.

5. Differential Scanning Calorimetry (DSC)

The differential scanning calorimetry (DSC) measurements were performed on an indium-calibrated Mettler-Toledo DSC822e equipped with a TSO801RO autosampler. The samples (weight range 1.0 – 2.6 mg) were placed in lidded 40 μL Al pans and thermally cycled twice under nitrogen with a heating/cooling rate of 10 °C/min. For the **ITIC-CX** samples, the reported data correspond to the first cycle and no thermal transitions were observed on second cycle. For the polymer samples, the reported data correspond to the second cycle. All data are reported endo up.

Table S3. Summary of DSC data for the **ITIC-CX** and donor polymers.

Material	T_{cp} (°C)[a]	T_c (°C)[b]	ΔH_c (kJ/mol)
ITIC-C3	-	-	-
ITIC-C6	204	195	36.2
ITIC-C9	168	162	15.8
PBDB-T	-	-	-
PBDB-TF	-	-	-

[a] peak maxima (endotherm) or minima (exotherm). [b] the onset temperature of the endotherm/exotherm.

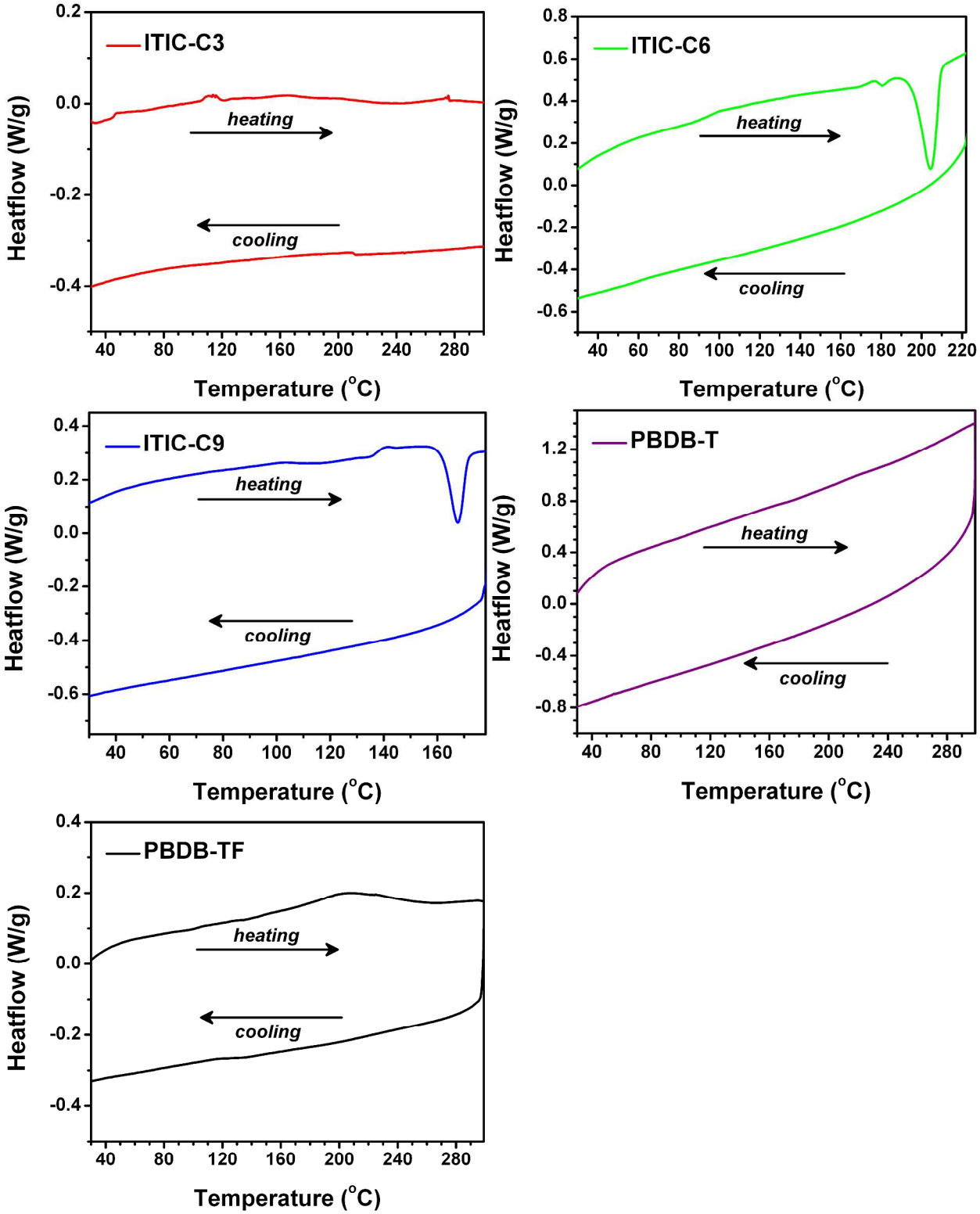

Figure S3. DSC heating and cooling traces of the **ITIC-CX** and donor polymers.

6. Thermogravimetric Analysis (TGA)

The thermogravimetric analysis measurements were performed on a TGA/SDTA-851e (Mettler Toledo) instrument equipped with a TS0801RO autosampler. The samples (weight range 2.0 – 3.0 mg) were heated with a rate of 10 °C/min under nitrogen.

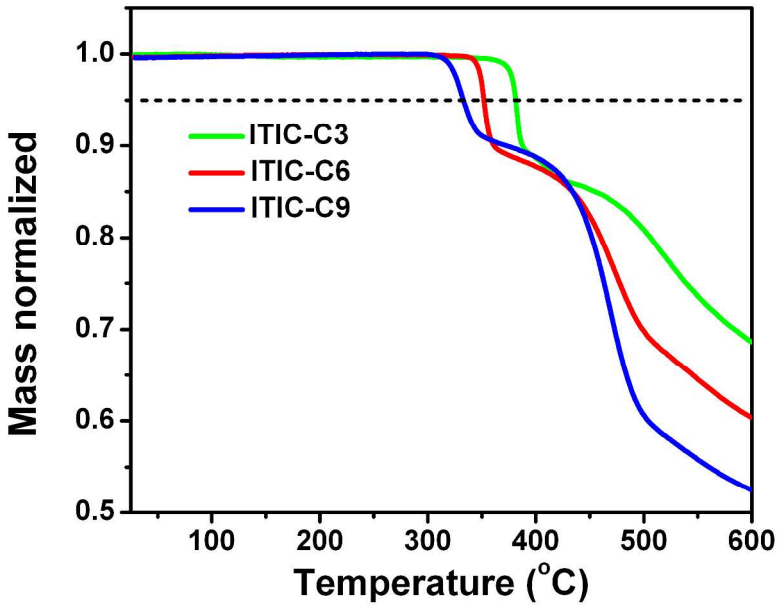

Figure S4. TGA heating traces of the **ITIC-CX**.

Table S4. Summary of TGA data for the **ITIC-CX**.

Material	T_d (°C)[a]
ITIC-C3	382
ITIC-C6	352
ITIC-C9	333

[a] Measured at the temperature corresponding to 5% mass loss of sample.

7. Gel Permeation Chromatography (GPC)

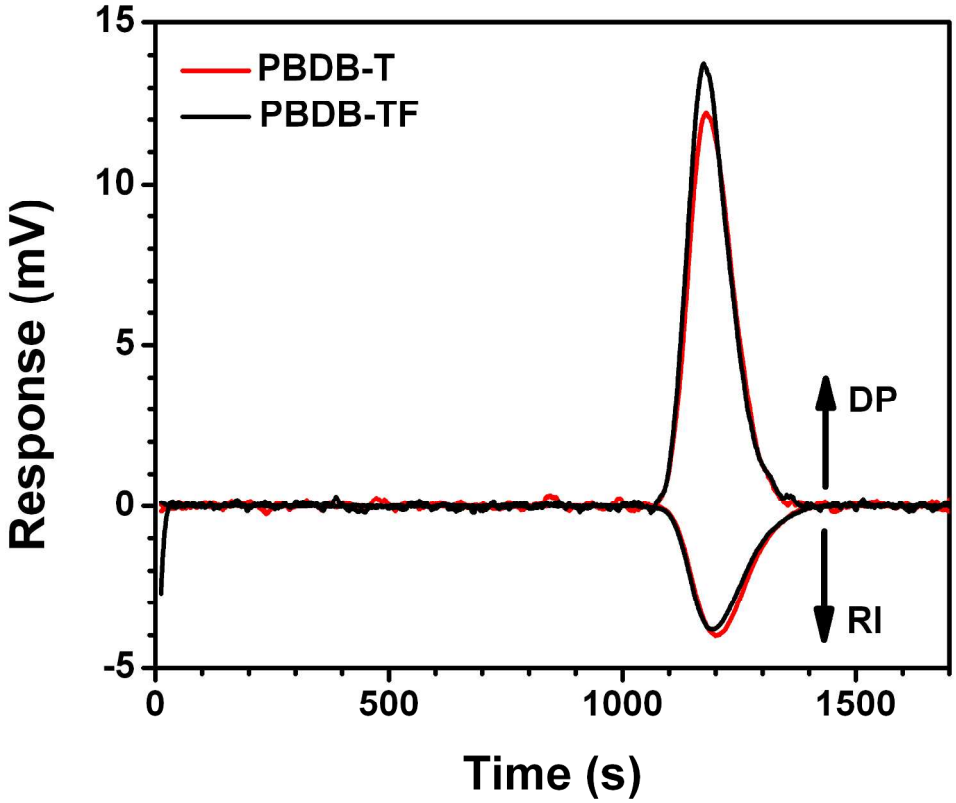

Figure S5. Gel Permeation Chromatography (GPC) traces of the donor polymers. Traces include data from refractive index (RI) and differential pressure (DP) detectors.

8. NMR Spectroscopy

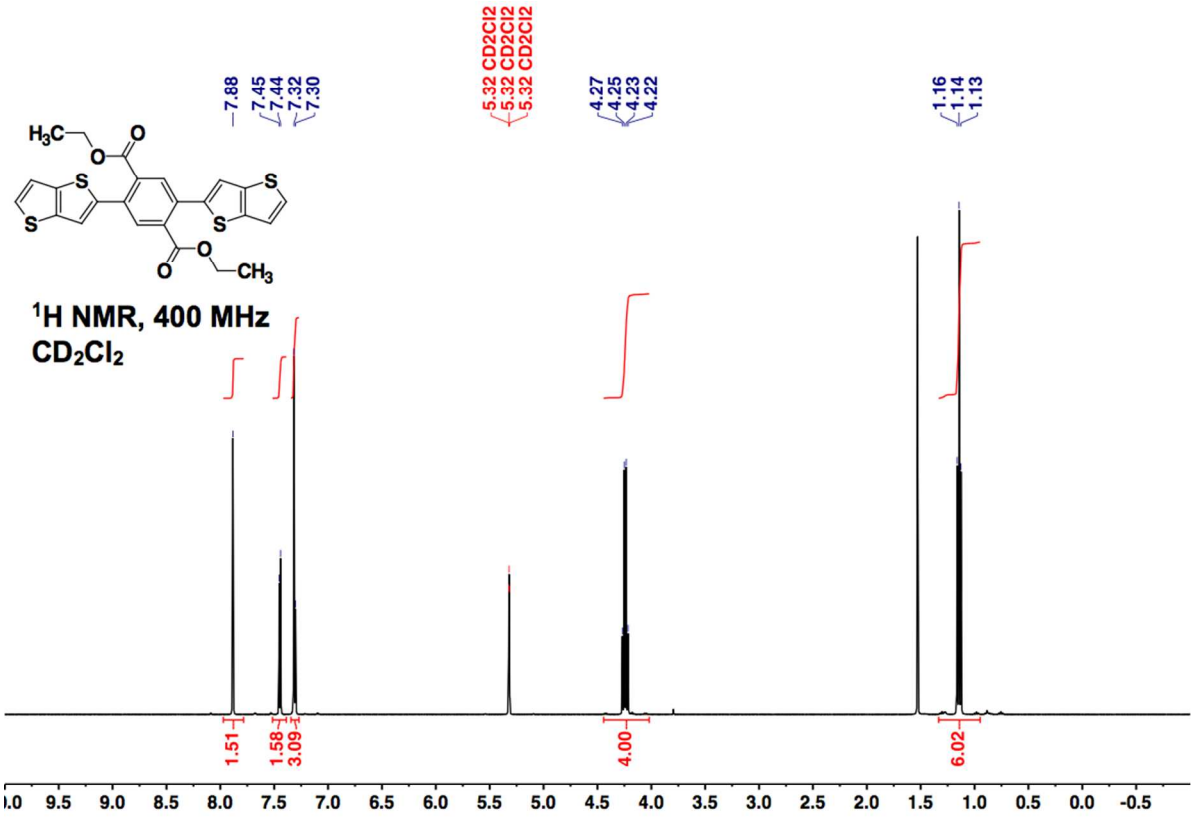

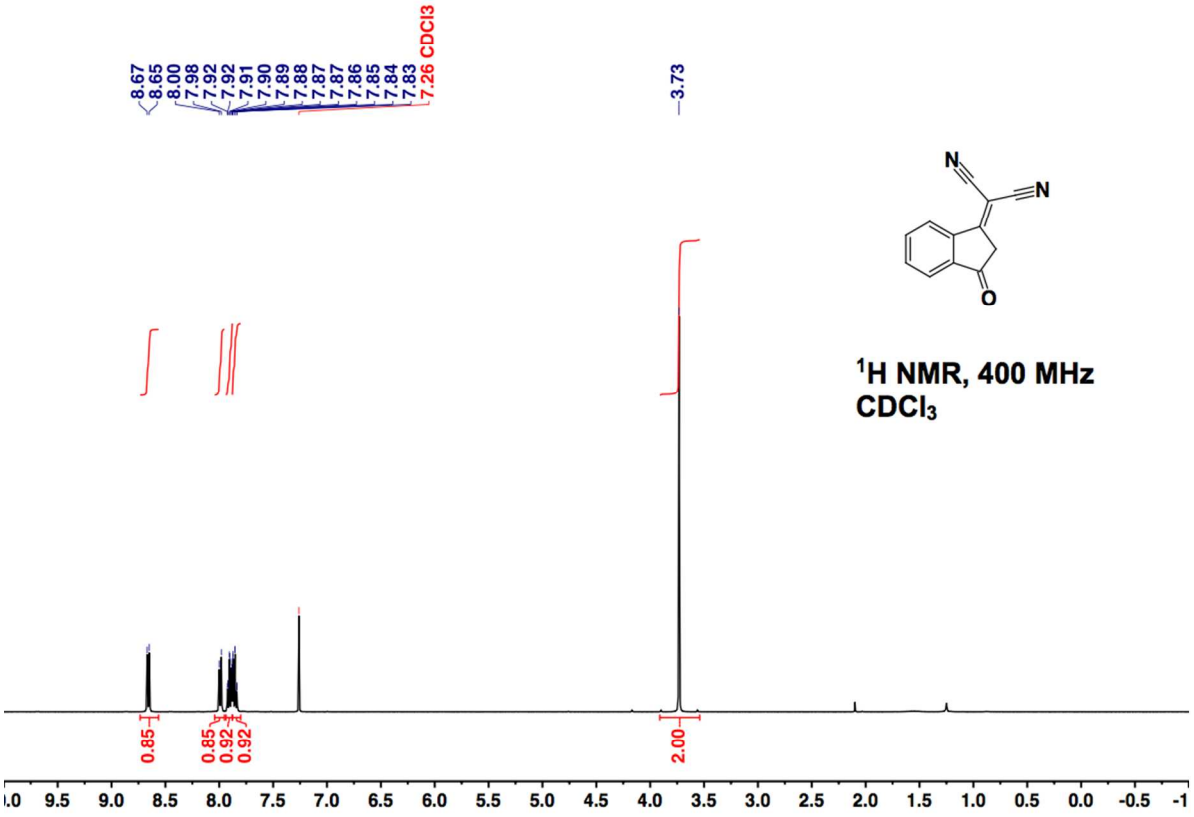

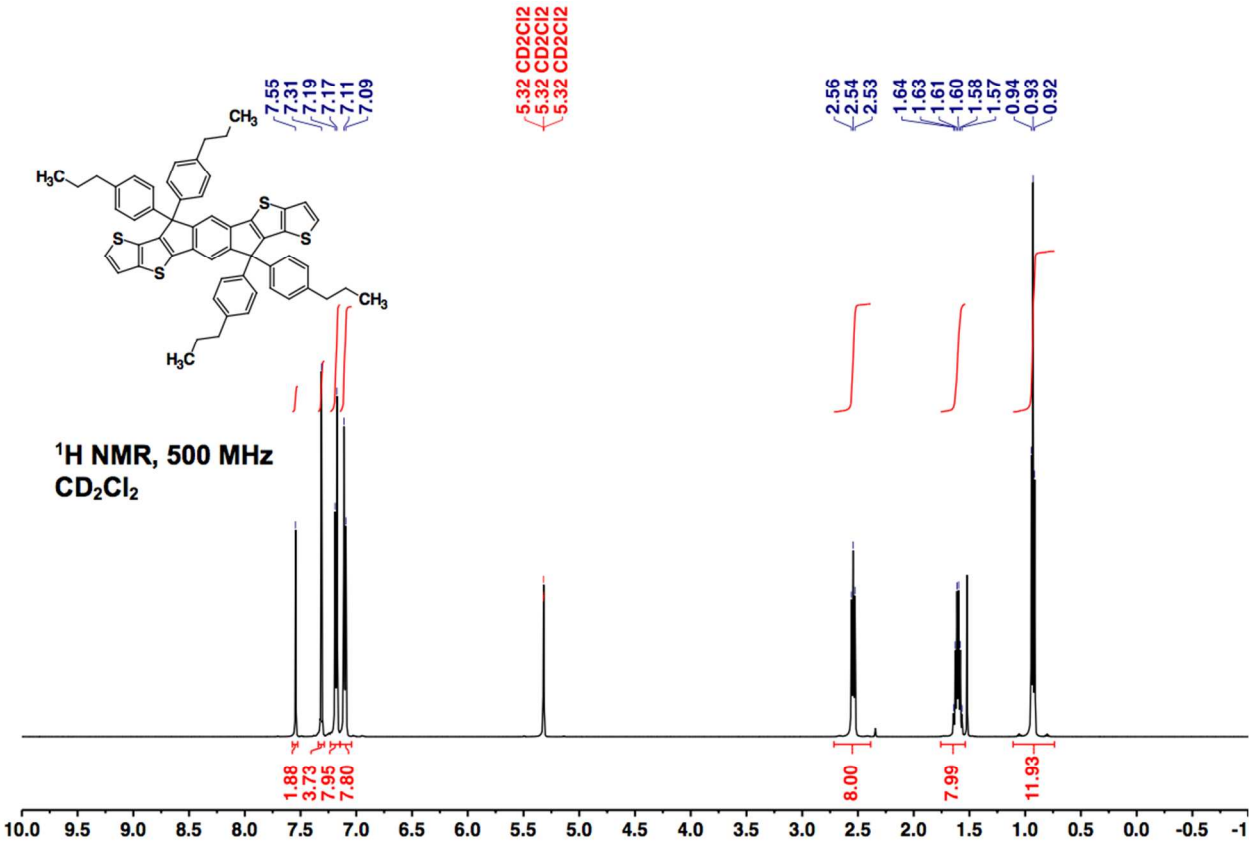
7.55
7.31
7.19
7.17
7.11
7.09
5.32 CD2Cl2
5.32 CD2Cl2
5.32 CD2Cl2
2.56
2.54
2.53
1.64
1.63
1.61
1.60
1.58
1.57
0.94
0.93
0.92
CH3
H3C
S
S
S
S
CH3
H3C
1H NMR, 500 MHz
CD2Cl2
1.88
3.73
7.95
7.80
8.00
7.99
11.93
10.0 9.5 9.0 8.5 8.0 7.5 7.0 6.5 6.0 5.5 5.0 4.5 4.0 3.5 3.0 2.5 2.0 1.5 1.0 0.5 0.0 -0.5 -1

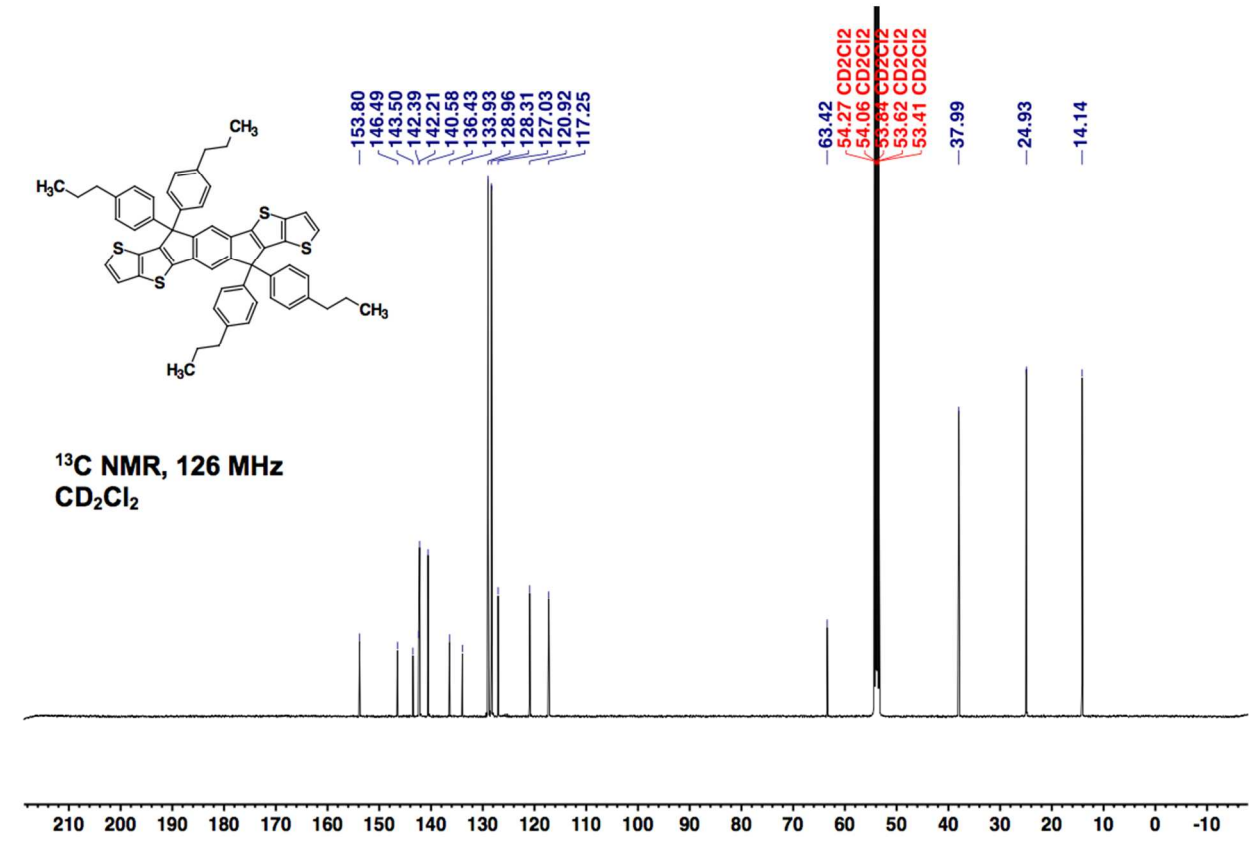
153.80
146.49
143.50
142.39
142.21
140.58
136.43
133.93
128.96
128.31
127.03
120.92
117.25
63.42
54.27 CD2Cl2
54.06 CD2Cl2
53.84 CD2Cl2
53.62 CD2Cl2
53.41 CD2Cl2
37.99
24.93
14.14
CH3
H3C
S
S
S
S
CH3
H3C
13C NMR, 126 MHz
CD2Cl2
210 200 190 180 170 160 150 140 130 120 110 100 90 80 70 60 50 40 30 20 10 0 -10

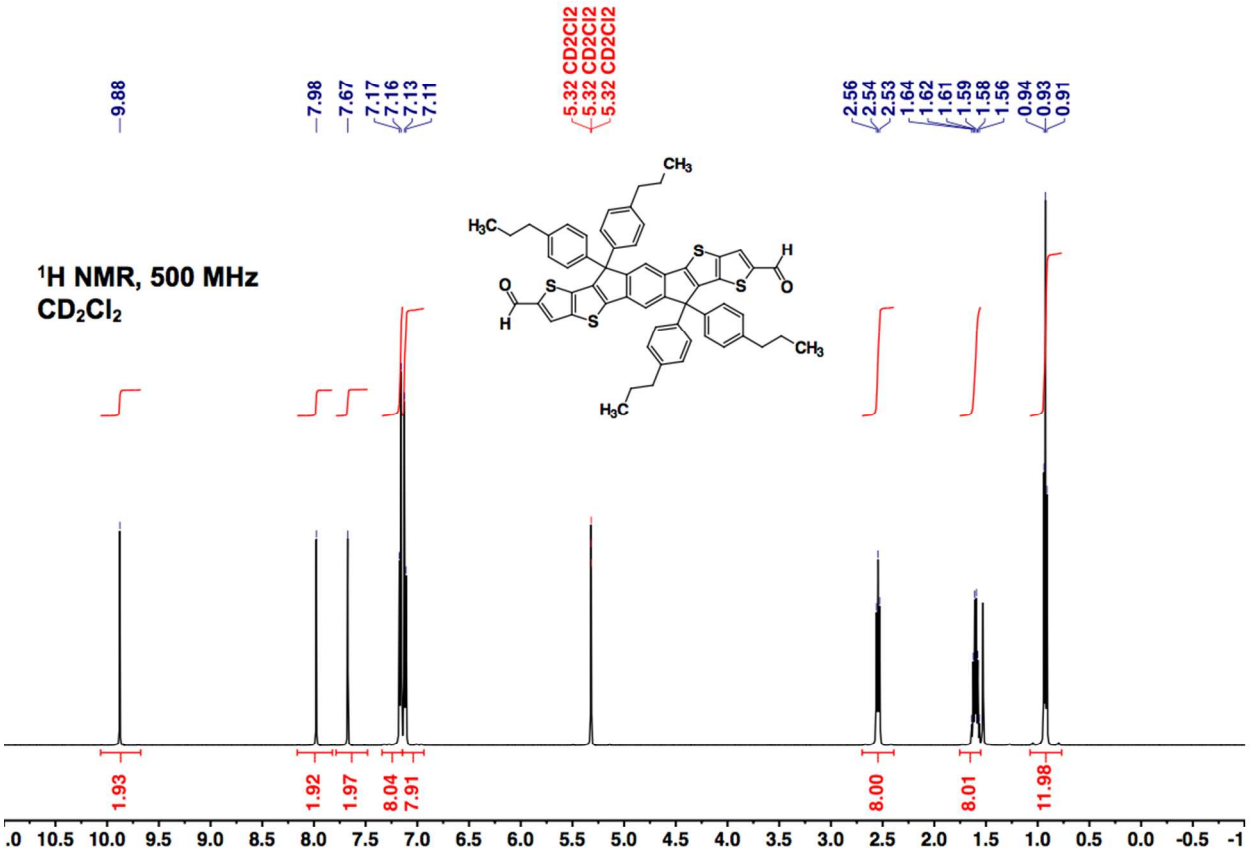
9.88
7.98
7.67
7.17
7.16
7.13
7.11
5.32 CD2Cl2
5.32 CD2Cl2
5.32 CD2Cl2
2.56
2.54
2.53
1.64
1.62
1.61
1.59
1.58
1.56
0.94
0.93
0.91
1H NMR, 500 MHz
CD2Cl2
1.93
1.92
1.97
8.04
7.91
8.00
8.01
11.98

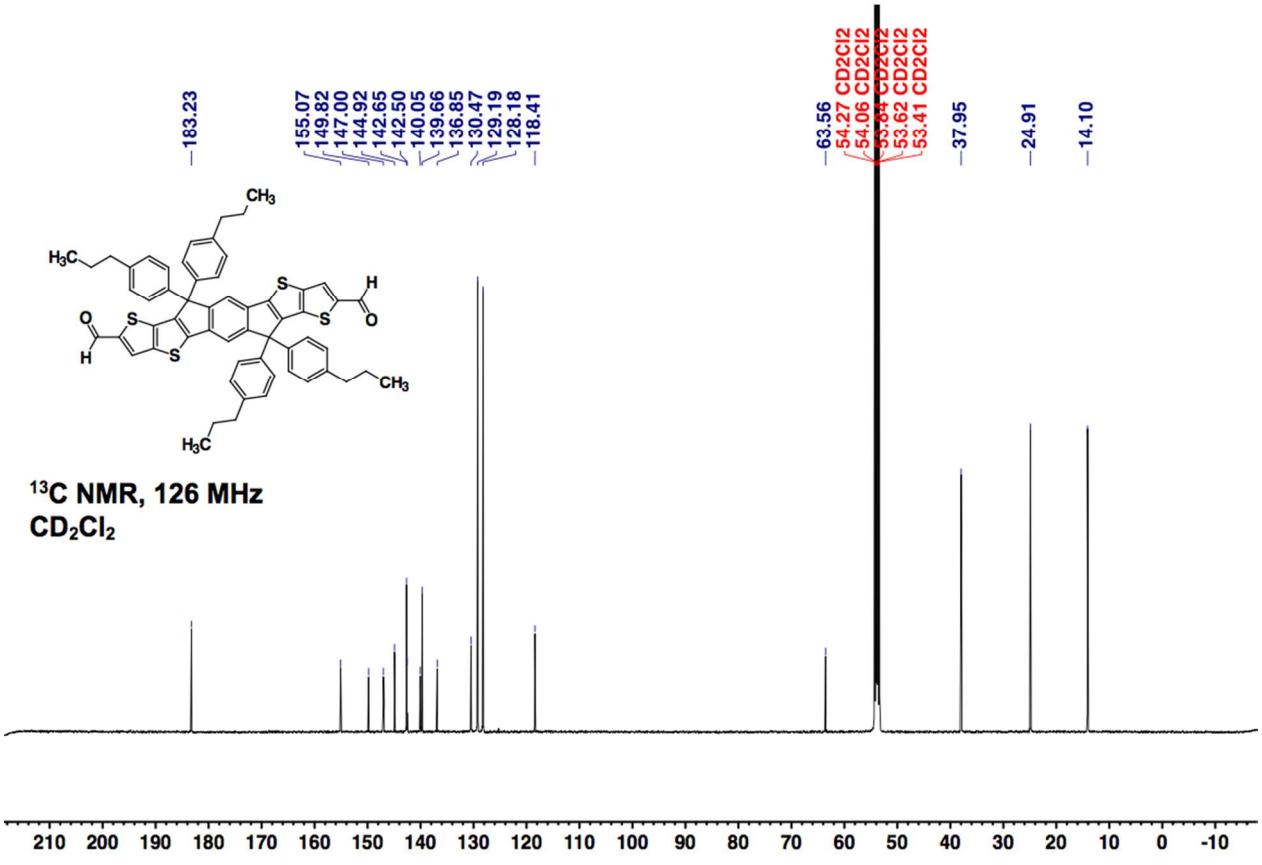
183.23
155.07
149.82
147.00
144.92
142.65
142.50
140.05
139.66
136.85
130.47
129.19
128.18
118.41
63.56
54.27 CD2Cl2
54.06 CD2Cl2
53.84 CD2Cl2
53.62 CD2Cl2
53.41 CD2Cl2
37.95
24.91
14.10
13C NMR, 126 MHz
CD2Cl2

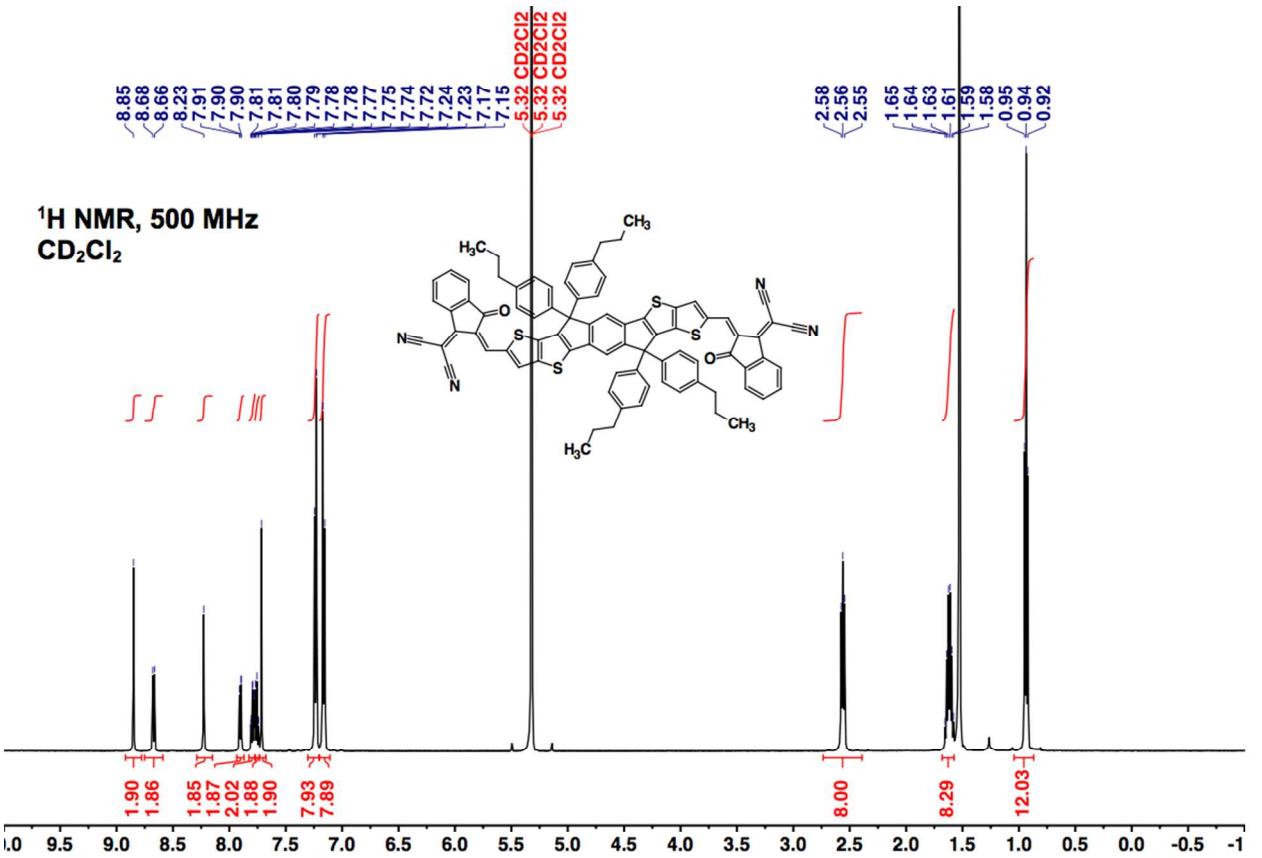
^{1}H NMR, 500 MHz
CD_2Cl_2

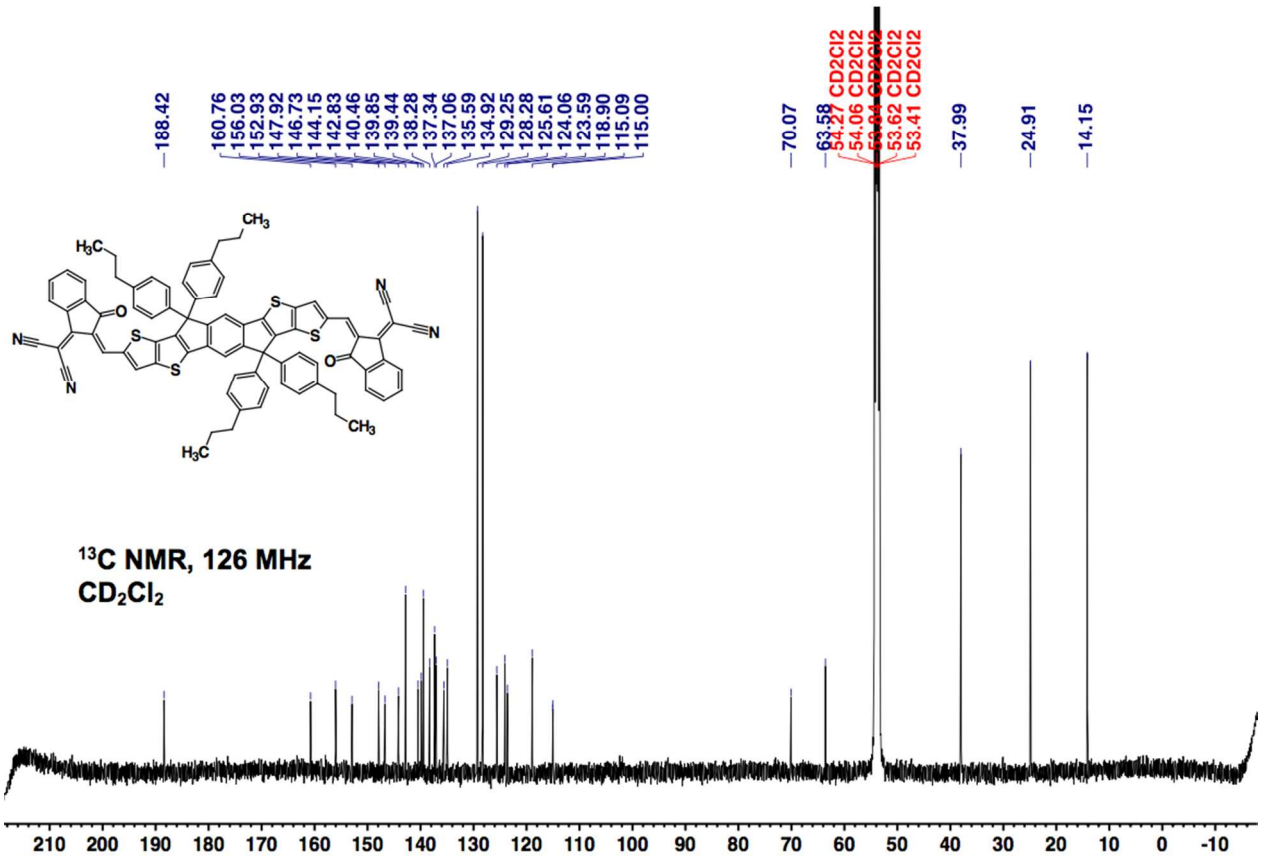
^{13}C NMR, 126 MHz
CD_2Cl_2

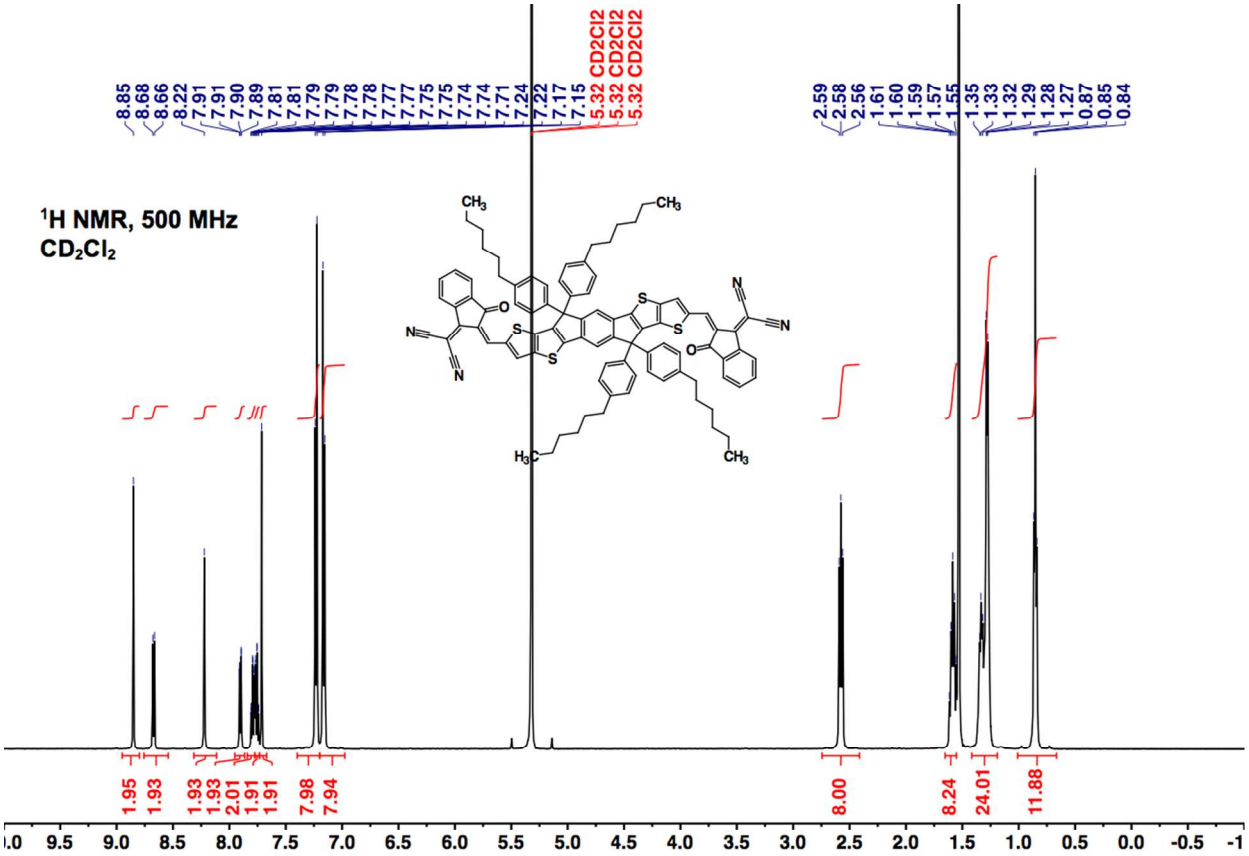
^{1}H NMR, 500 MHz
CD_2Cl_2

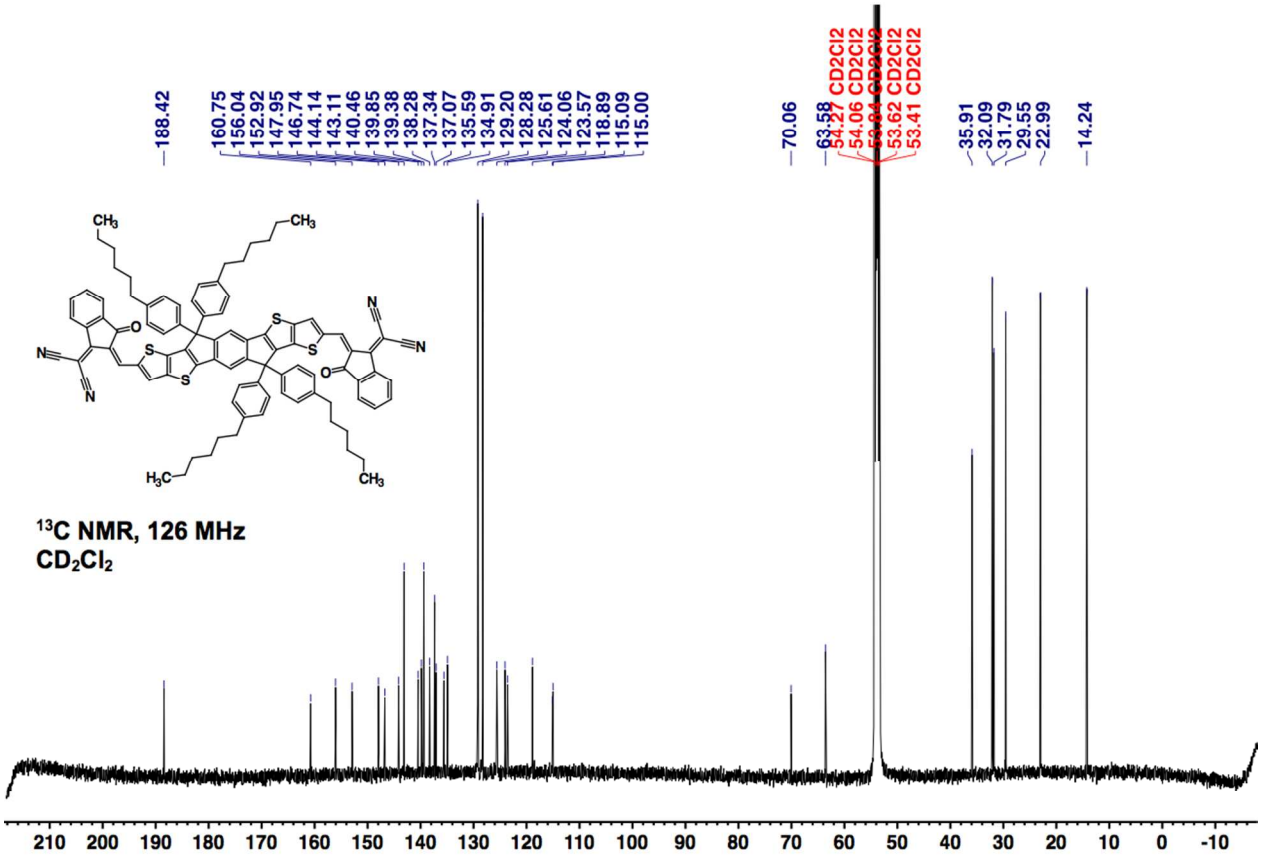
^{13}C NMR, 126 MHz
CD_2Cl_2

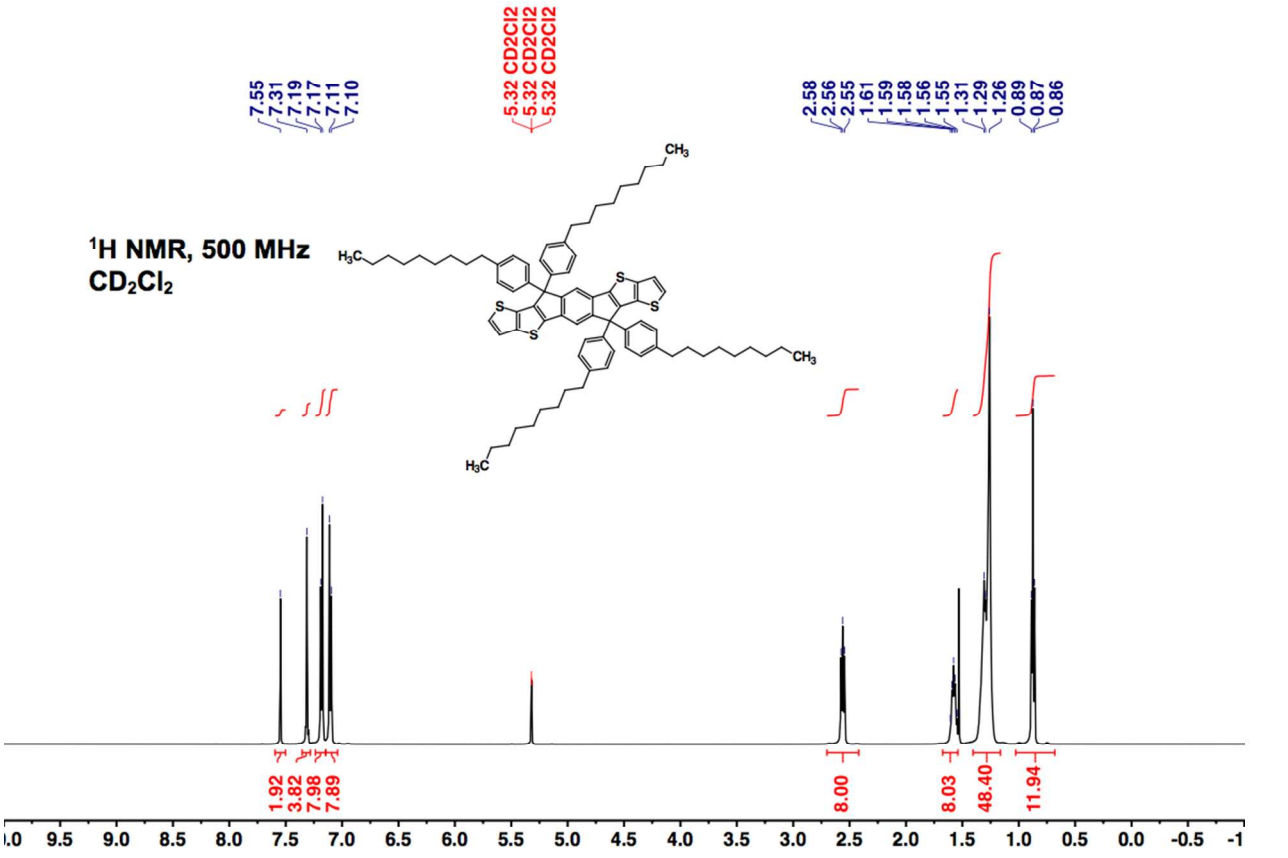
7.55
7.31
7.19
7.17
7.11
7.10
5.32 CD2Cl2
5.32 CD2Cl2
5.32 CD2Cl2
2.58
2.56
2.55
1.61
1.59
1.58
1.56
1.55
1.31
1.29
1.26
0.89
0.87
0.86
1H NMR, 500 MHz
CD2Cl2
1.92
3.82
7.98
7.89
8.00
8.03
48.40
11.94

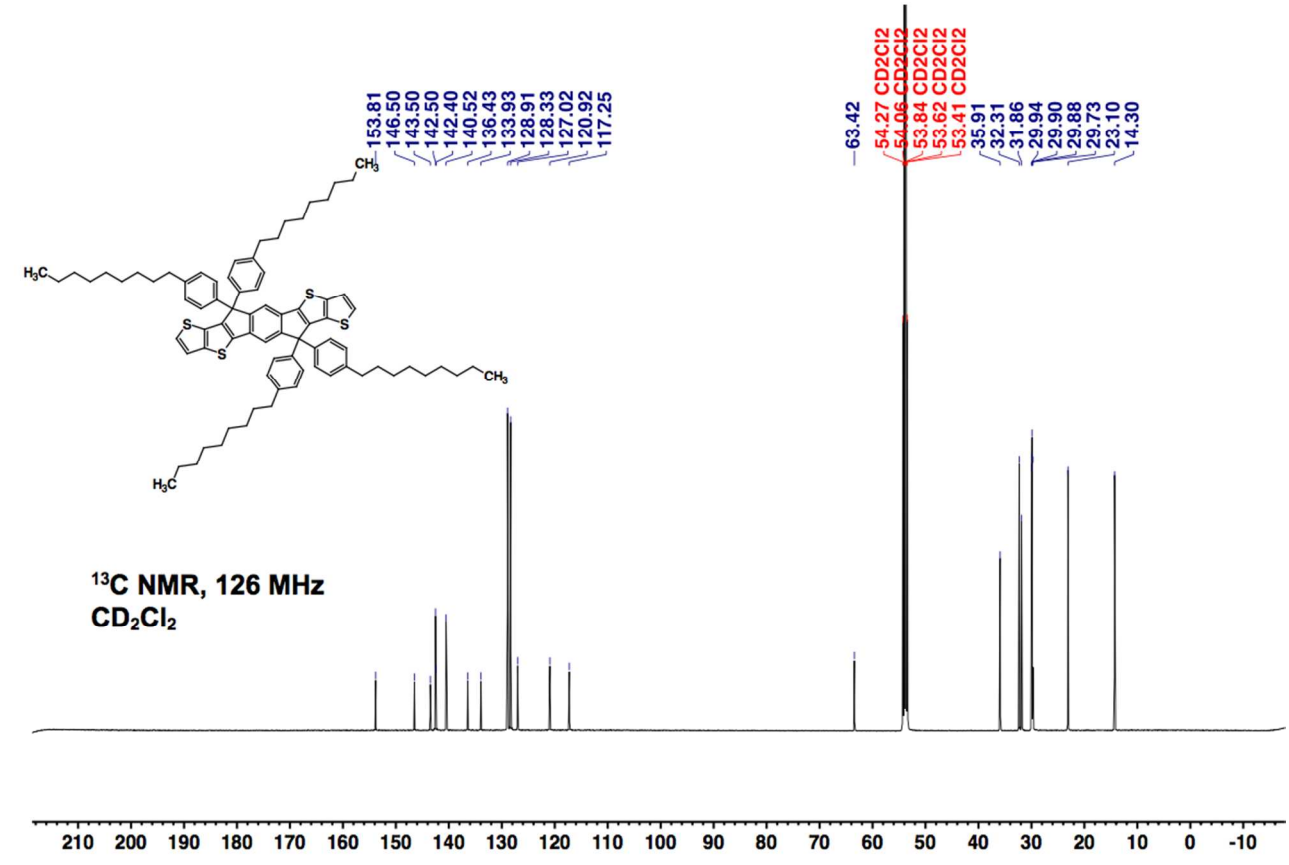
153.81
146.50
143.50
142.50
142.40
140.52
136.43
133.93
128.91
128.33
127.02
120.92
117.25
63.42
54.27 CD2Cl2
54.06 CD2Cl2
53.84 CD2Cl2
53.62 CD2Cl2
53.41 CD2Cl2
35.91
32.31
31.86
29.94
29.90
29.88
29.73
23.10
14.30
13C NMR, 126 MHz
CD2Cl2

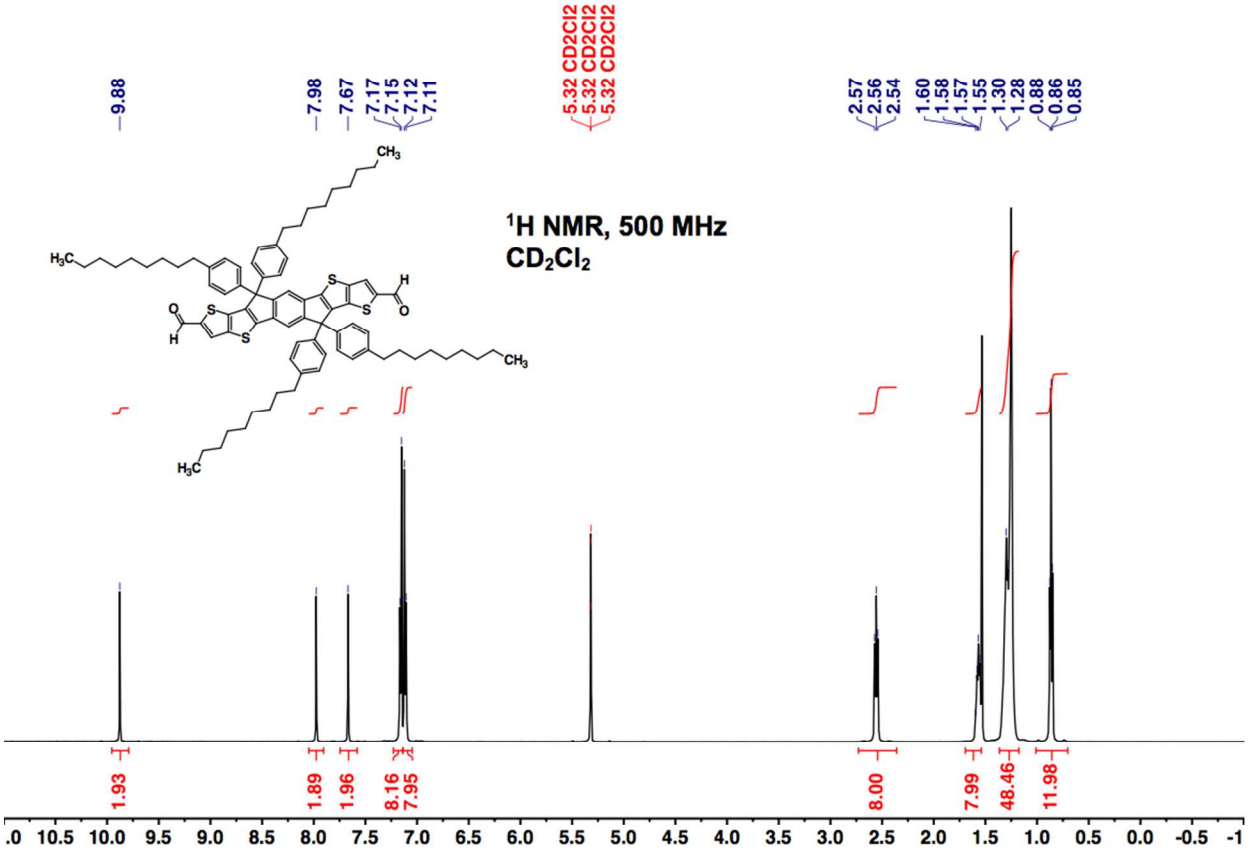
9.88
7.98
7.67
7.17
7.15
7.12
7.11
5.32 CD2Cl2
5.32 CD2Cl2
5.32 CD2Cl2
2.57
2.56
2.54
1.60
1.58
1.57
1.55
1.30
1.28
0.88
0.86
0.85
1H NMR, 500 MHz
CD2Cl2
1.93
1.89
1.96
8.16
7.95
8.00
7.99
48.46
11.98
10.5 10.0 9.5 9.0 8.5 8.0 7.5 7.0 6.5 6.0 5.5 5.0 4.5 4.0 3.5 3.0 2.5 2.0 1.5 1.0 0.5 0.0 -0.5 -1

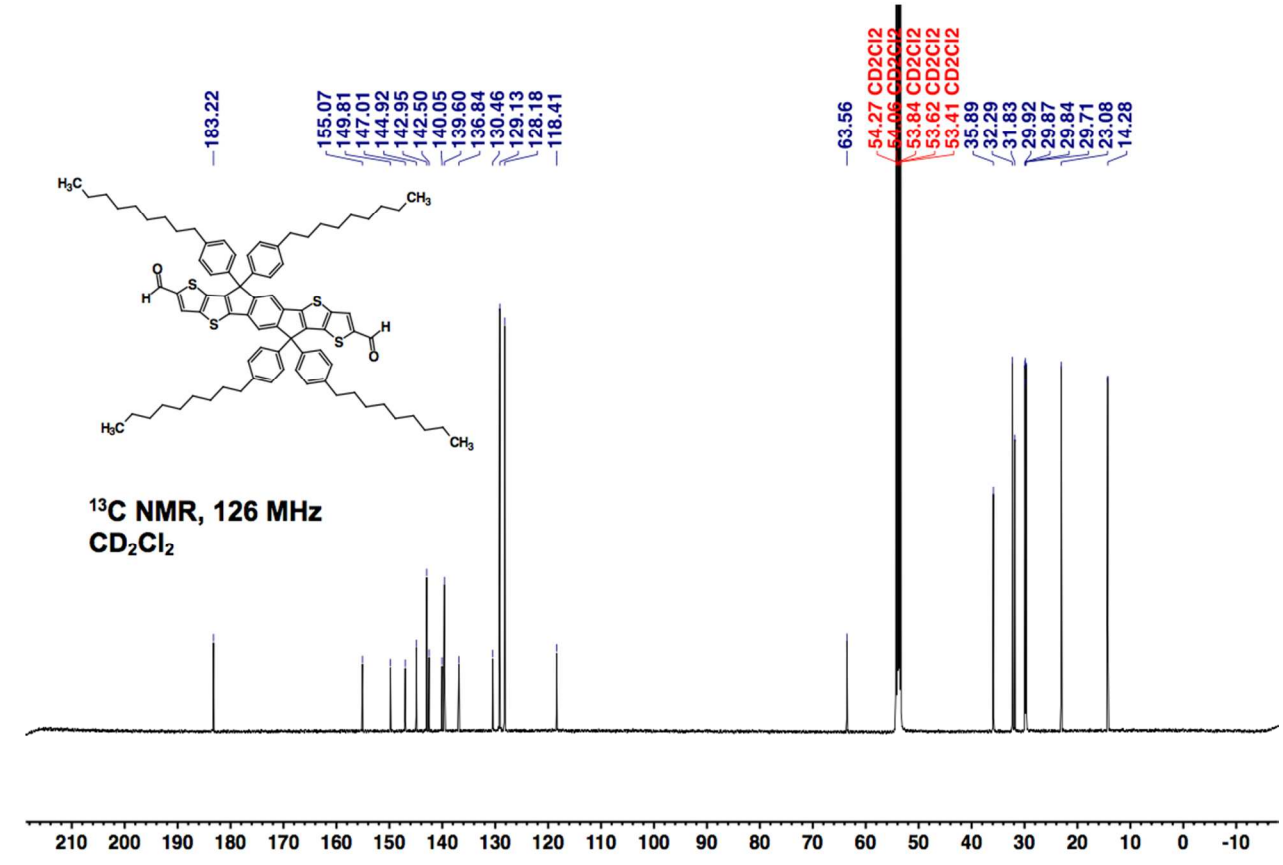
183.22
155.07
149.81
147.01
144.92
142.95
142.50
140.05
139.60
136.84
130.46
129.13
128.18
118.41
63.56
54.27 CD2Cl2
54.06 CD2Cl2
53.84 CD2Cl2
53.62 CD2Cl2
53.41 CD2Cl2
35.89
32.29
31.83
29.92
29.87
29.84
29.71
23.08
14.28
13C NMR, 126 MHz
CD2Cl2
210 200 190 180 170 160 150 140 130 120 110 100 90 80 70 60 50 40 30 20 10 0 -10

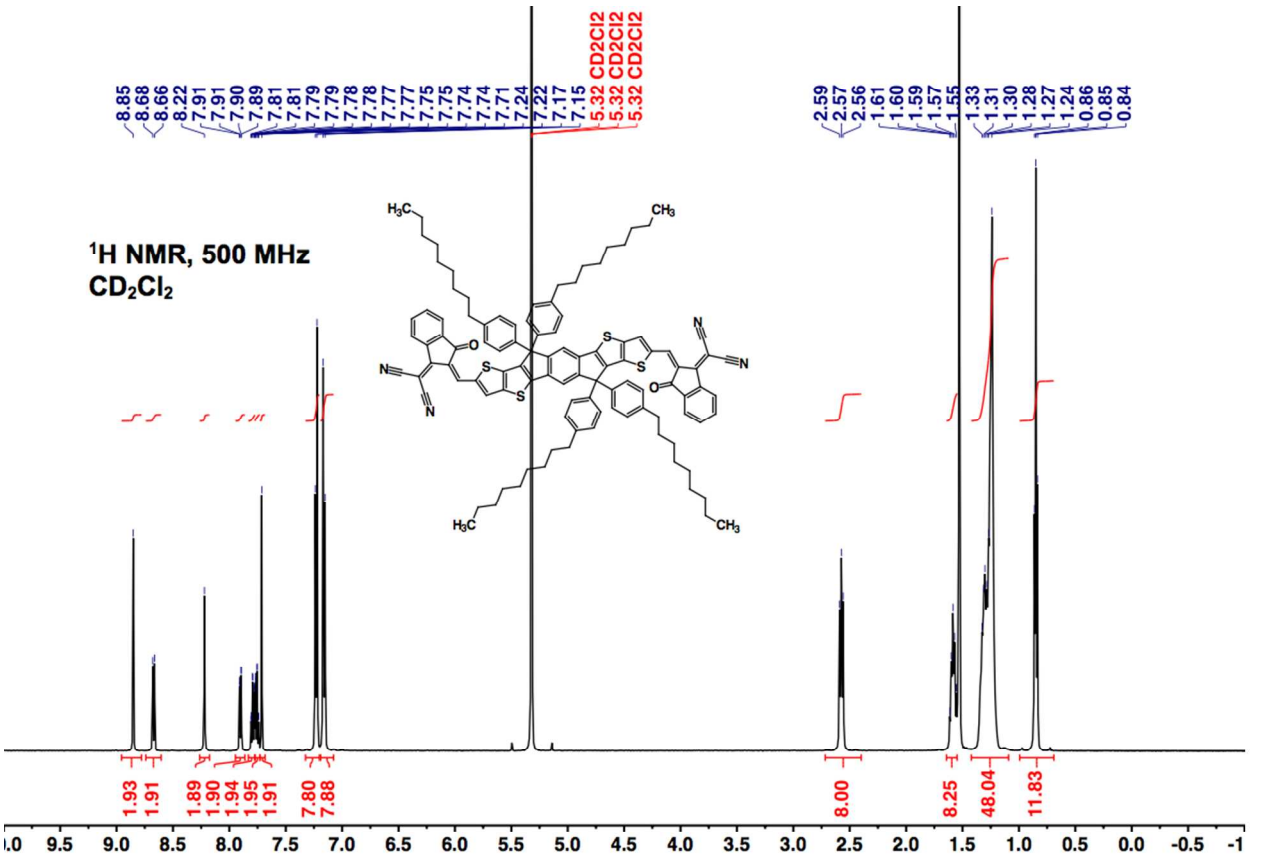
^{1}H NMR, 500 MHz
CD_2Cl_2

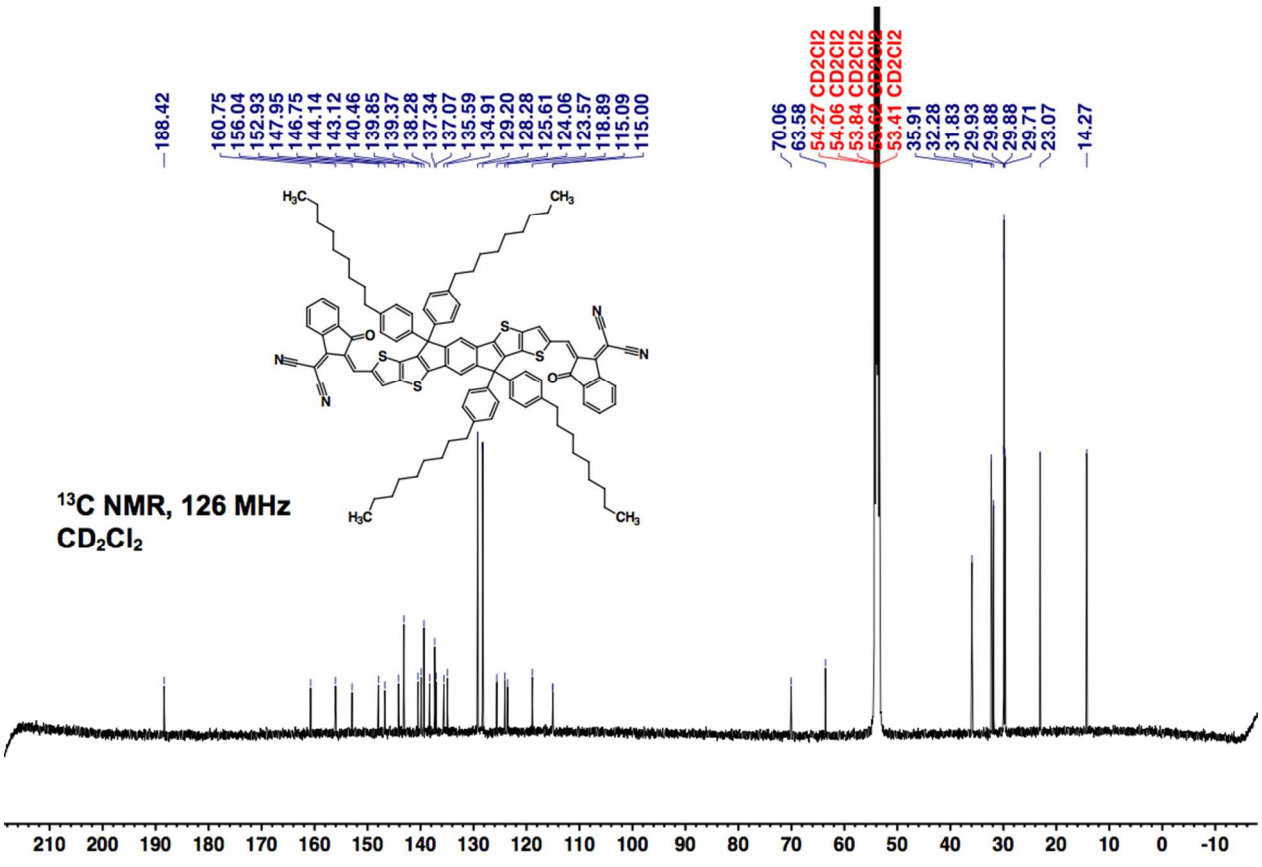
^{13}C NMR, 126 MHz
CD_2Cl_2

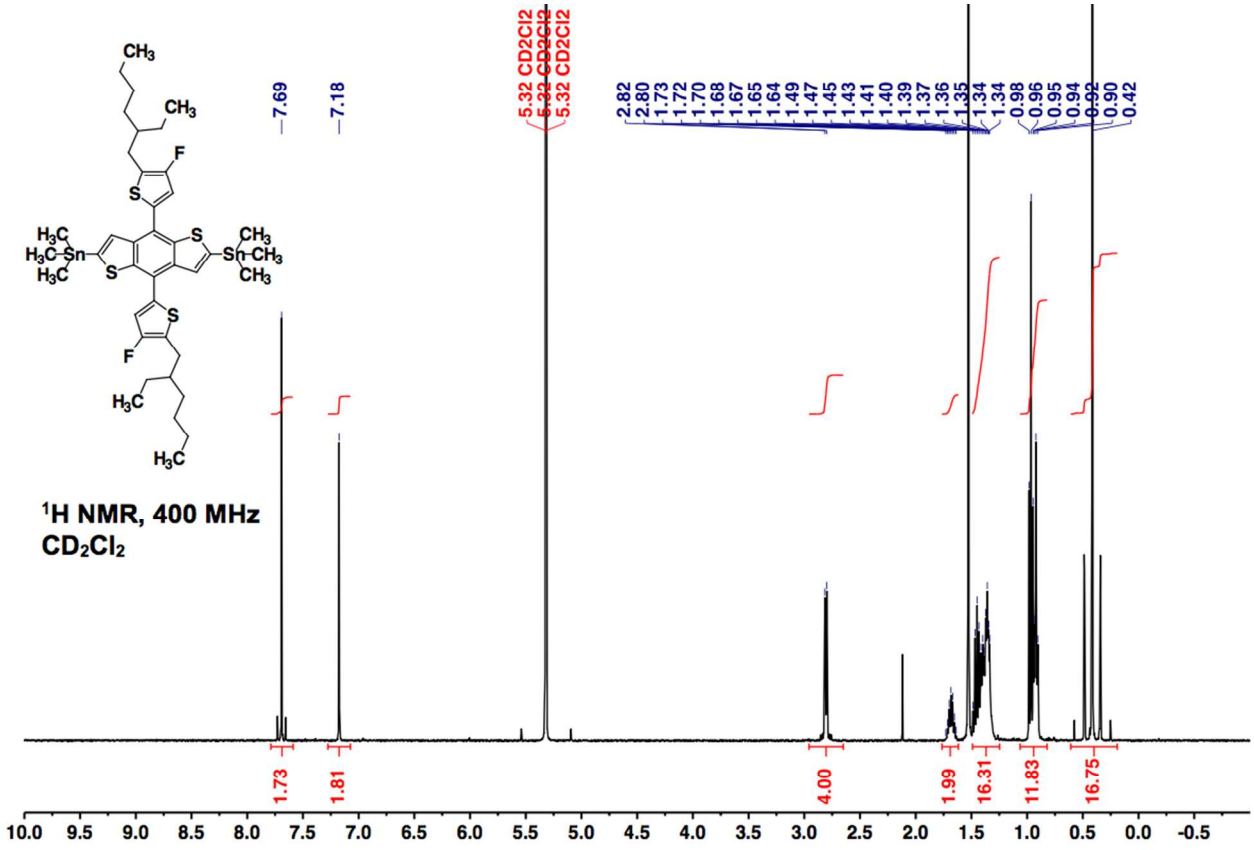
7.69
7.18
5.32 CD2Cl2
2.82
2.80
1.73
1.72
1.70
1.68
1.67
1.65
1.64
1.49
1.47
1.45
1.43
1.41
1.40
1.39
1.37
1.36
1.35
1.34
1.34
0.98
0.96
0.95
0.94
0.92
0.90
0.42
1.73
1.81
4.00
1.99
16.31
11.83
16.75
10.0 9.5 9.0 8.5 8.0 7.5 7.0 6.5 6.0 5.5 5.0 4.5 4.0 3.5 3.0 2.5 2.0 1.5 1.0 0.5 0.0 -0.5
1H NMR, 400 MHz
CD2Cl2

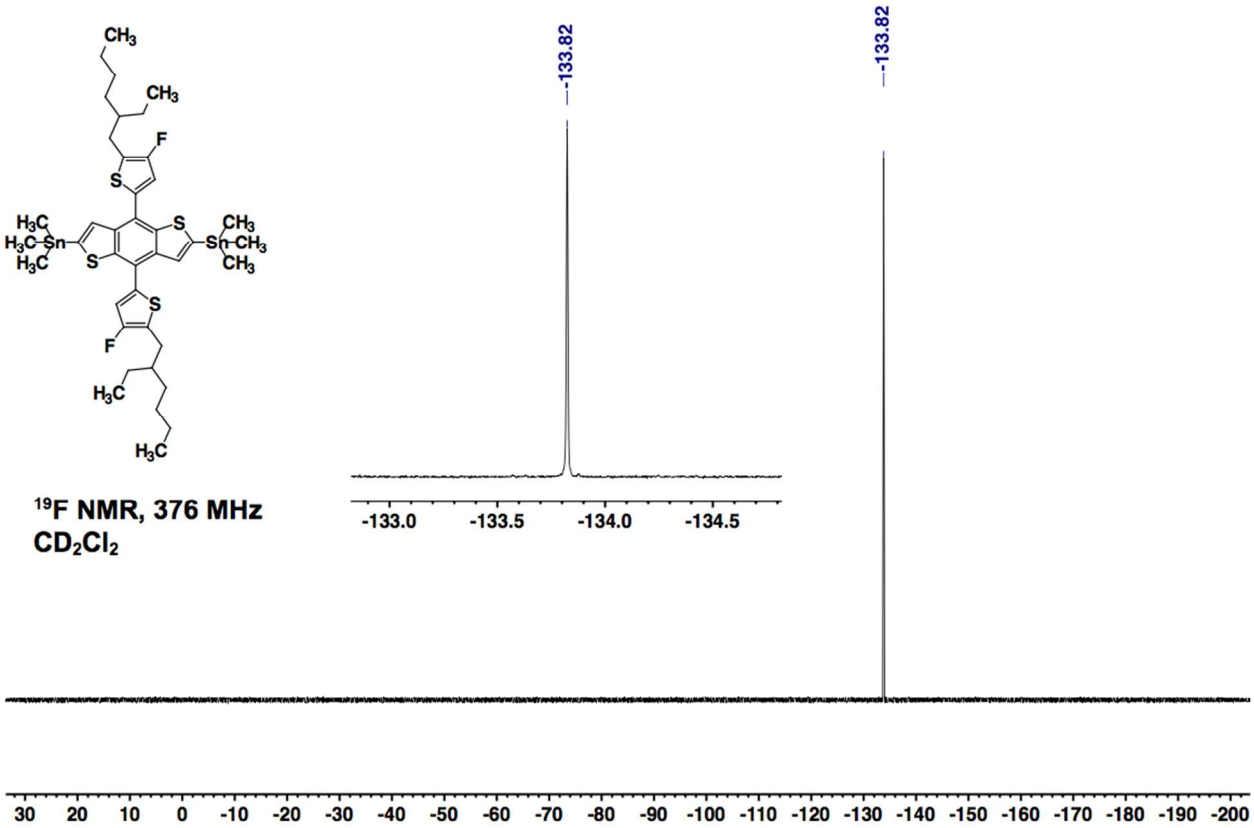
-133.82
-133.82
-133.0 -133.5 -134.0 -134.5
19F NMR, 376 MHz
CD2Cl2
30 20 10 0 -10 -20 -30 -40 -50 -60 -70 -80 -90 -100 -110 -120 -130 -140 -150 -160 -170 -180 -190 -200

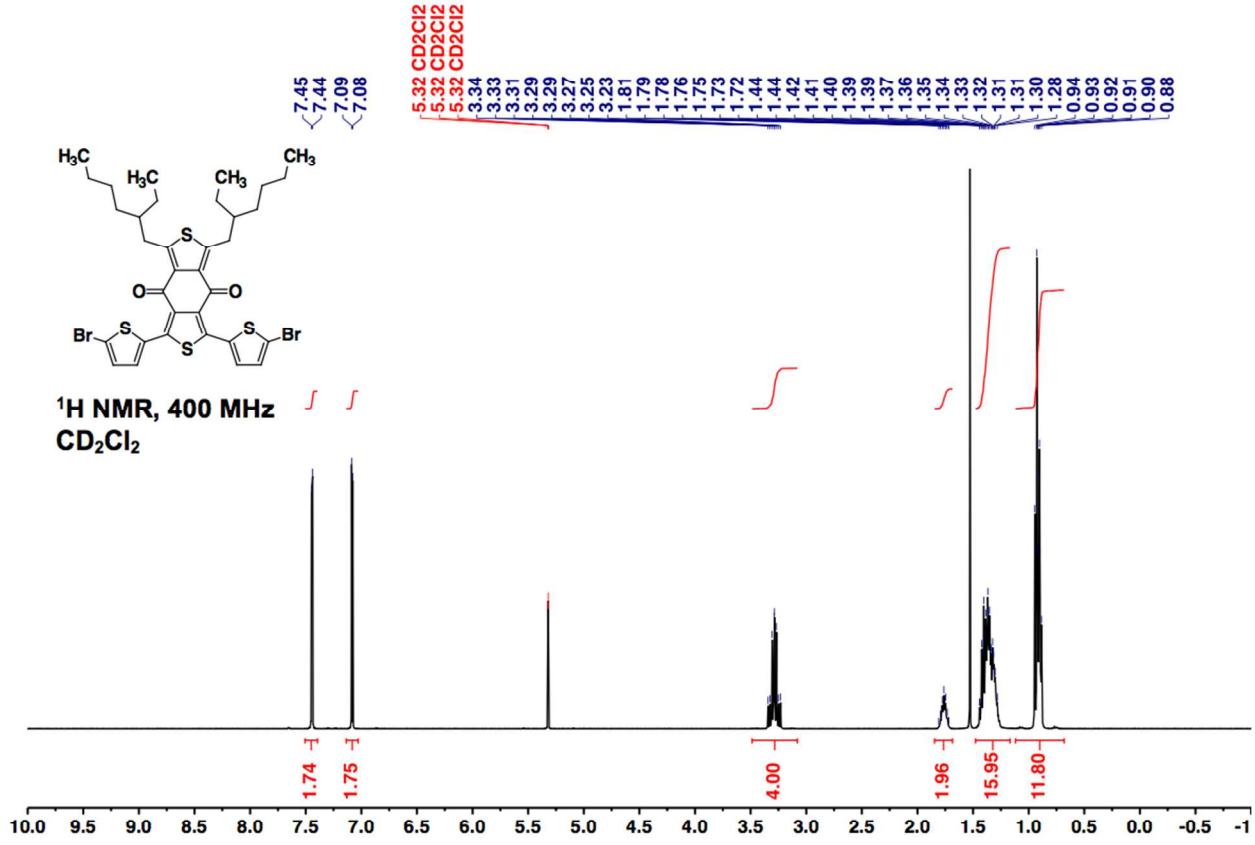
1H NMR, 400 MHz
CD2Cl2

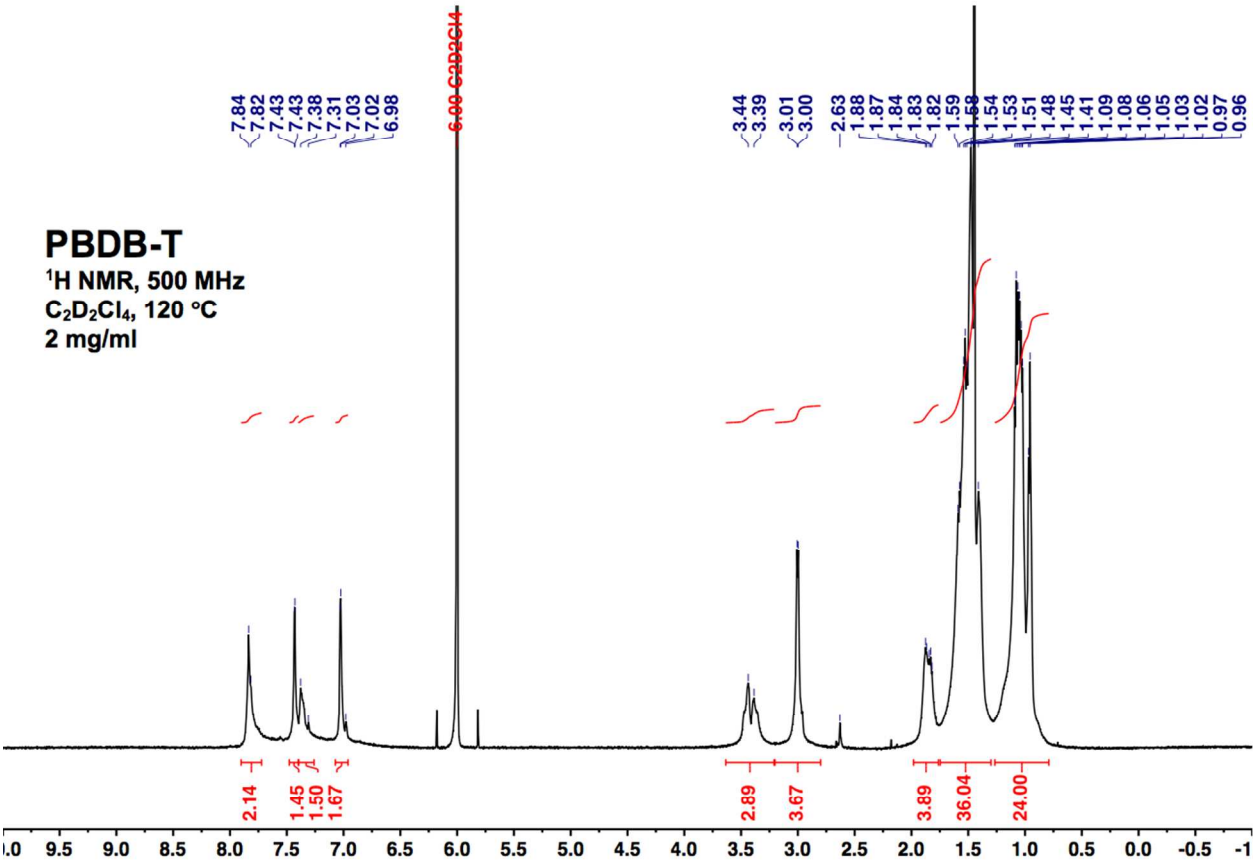
PBDB-T
1H NMR, 500 MHz
C2D2Cl4, 120 °C
2 mg/ml

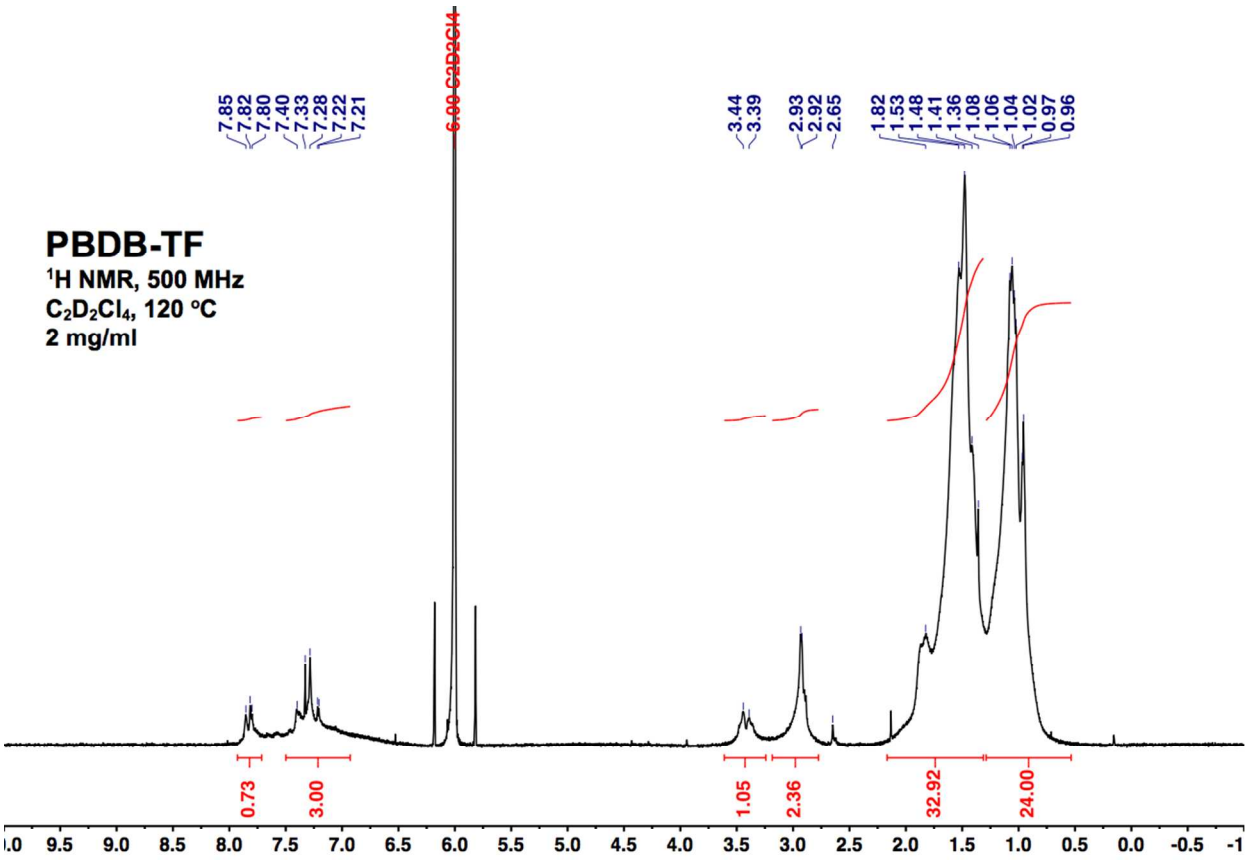
PBDB-TF
1H NMR, 500 MHz
C2D2Cl4, 120 °C
2 mg/ml
7.85
7.82
7.80
7.40
7.33
7.28
7.22
7.21
6.00 C2D2Cl4
3.44
3.39
2.93
2.92
2.65
1.82
1.53
1.48
1.41
1.36
1.08
1.06
1.04
1.02
0.97
0.96
0.73
3.00
1.05
2.36
32.92
24.00

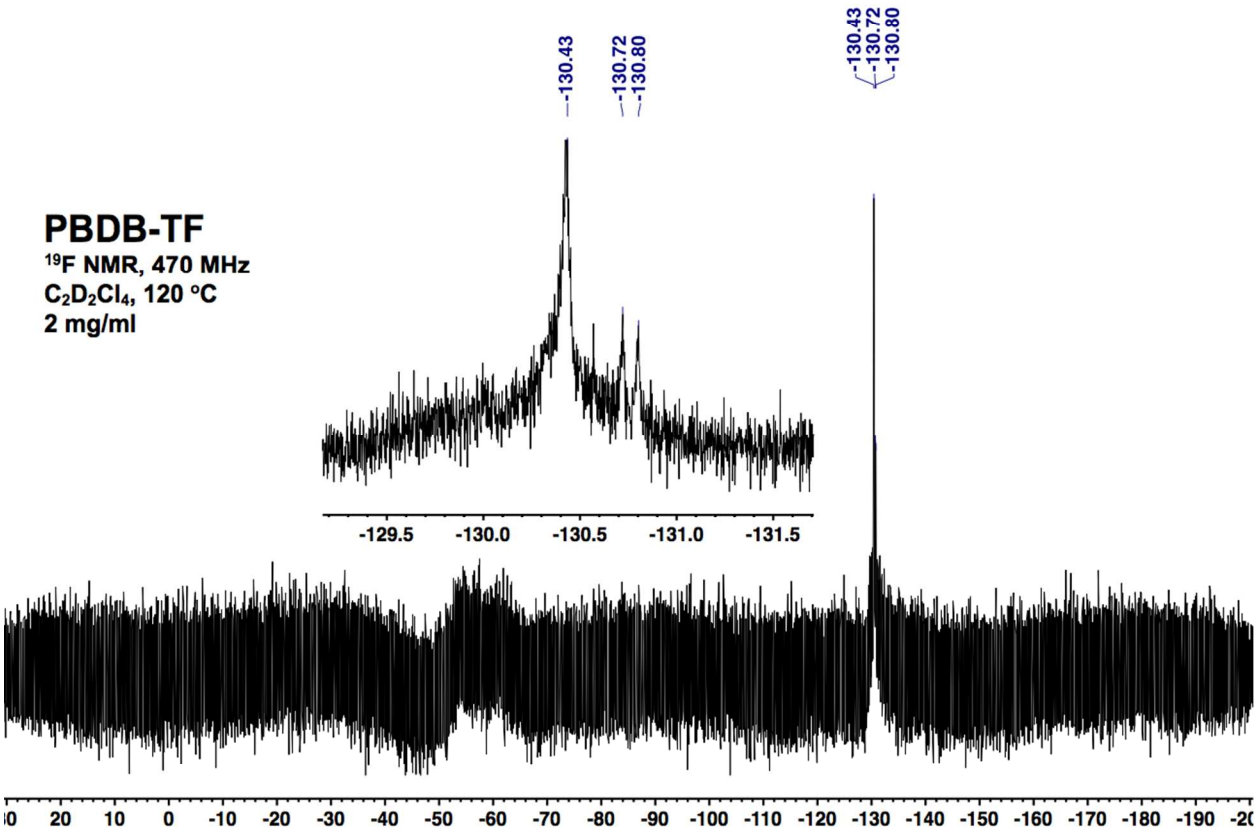
PBDB-TF
19F NMR, 470 MHz
C2D2Cl4, 120 °C
2 mg/ml
-130.43
-130.72
-130.80
-129.5
-130.0
-130.5
-131.0
-131.5

9. Solar Cell Device Fabrication and Characterization

An "inverted" device architecture, indium tin oxide (ITO)/ZnO/copolymer:ITIC-CX/MoO_3/Ag, was used. Pre-patterned ITO-coated glass wafers (Thin Film Devices, Inc.) with a thickness of ~280 nm and sheet resistance of ~20 Ω/sq were used as substrates. ITO electrodes were cleaned by sequential sonication in aqueous detergent solution, deionized water, methanol, acetone, and isopropanol. Finally, the ITO electrodes were cleaned with a UV/ozone treatment (Jelight Co.) for 15 min. The cathode interfacial layer, ZnO, was deposited from a precursor solution of 0.5 M zinc acetate dihydrate and 0.5 M 2-aminoethanol in 2-methoxyethanol, which was spun cast at 7000 rpm for 30 s and annealed at 170 °C for 10 min in air. Active layer solutions were prepared by dissolving copolymer and **ITIC-CX** (1:1 weight ratio) in a chlorobenzene:1,8-diiodooctane (99:1 v/v) solvent mixture (10.0 mg mL^{-1} copolymer concentration) with vigorous stirring for 12 h at 70 °C in an argon-filled glovebox. Active layer solutions were then cooled to ~25 °C over 10 min. and then active layers were spun cast inside glovebox (2500 rpm, 60 s). Substrates were then annealed at 160 °C for 10 min. inside glovebox. Thin layers of 9 nm MoO_3 and 100 nm of Ag were then thermally evaporated through a shadow mask at ~10^{-6} Torr.

The photovoltaic characteristics of devices were tested in air. The current density-voltage (*J*–*V*) curves were obtained by a Keithley 2400 source-measure unit using four-point contact measurements. The photocurrent was measured under simulated AM1.5G irradiation (100 mW cm^{-2}) using Xe arc lamp of a Spectra-Nova 300W Class-A solar simulator. The light intensity was calibrated using an NREL-certified monocrystalline Si photodiode coupled to a KG3 filter to bring the spectral mismatch to unity. The area of all devices was 6 mm^2. External quantum efficiency (EQE) was measured using Newport QE-PV-SI setup. Incident light from a Xe lamp (300 W) passing through a monochromator (Newport, Cornerstone 260) was focused on the active area of the cell. The output current was measured using a current pre-amplifier (Newport, 70710QE) and a lock-in amplifier (Newport, 70105 Dual channel Merlin). A calibrated silicon diode (Newport 70356) was used as a reference.

Table S5. Photovoltaic parameters for donor polymer:**ITIC-CX** solar cells.

Blend	Thermal Annealing Temp. (°C)	V_{OC} (V)	J_{SC} (mA/cm^2)	J_{SC} (mA/cm^2)[a]	FF (%)	PCE (%)	# of devices
PBDB-T: ITIC-C3	-	0.86 ± 0.02 (0.88)	1.75 ± 0.18 (2.02)	1.64 ± 0.10 (1.64)	43.7 ± 2.5 (47.1)	0.66 ± 0.12 (0.83)	4
	160	0.31 ± 0.19 (0.43)	0.56 ± 0.31 (0.64)	0.53 ± 0.03 (0.54)	29.1 ± 7.4 (41.9)	0.06 ± 0.03 (0.12)	9
PBDB-TF: ITIC-C3	160	0.04 ± 0.02 (0.05)	0.58 ± 0.10 (0.53)	0.54 ± 0.02 (0.56)	22.4 ± 11.4 (35.3)	0.006 ± 0.004 (0.011)	6
PBDB-T: ITIC-C6	-	0.90 ± 0.01 (0.89)	15.9 ± 0.5 (16.5)	15.5 ± 0.13 (15.6)	62.0 ±0.3 (61.6)	8.80 ± 0.23 (9.16)	11
	160	0.87 ± 0.01 (0.88)	14.9 ±0.7 (13.7)	15.6 ± 0.2 (15.6)	65.0 ± 1.5 (67.1)	8.77 ± 0.25 (9.18)	65
	190	0.85 ± 0.01 (0.86)	15.0 ± 0.1 (15.1)	15.0 ± 0.1 (15.1)	64.3 ± 0.9 (65.8)	8.22 ± 0.18 (8.52)	8
PBDB-TF: ITIC-C6	-	1.01 ± 0.01 (1.01)	14.3 ± 0.10 (14.3)	14.3 ± 0.10 (14.3)	59.6 ± 1.0 (60.4)	8.56 ± 0.18 (8.78)	8
	160	0.98 ± 0.01 (0.99)	13.5 ± 0.9 (15.3)	14.3 ± 0.14 (14.5)	63.9 ± 1.6 (62.0)	9.05 ± 0.16 (9.31)	17
	190	0.97 ± 0.01 (0.98)	14.1 ± 0.2 (14.3)	14.1 ± 0.2 (14.3)	65.7 ± 0.4 (66.5)	9.05 ± 0.22 (9.36)	7
PBDB-T: ITIC-C9	-	0.92 ± 0.01 (0.92)	15.4 ± 0.10 (15.5)	15.4 ± 0.10 (15.5)	61.7 ± 0.3 (61.8)	8.74 ± 0.05 (8.82)	7
	160	0.87 ± 0.01 (0.89)	14.1 ± 0.7 (15.0)	15.1 ± 0.13 (15.2)	68.7 ± 1.1 (70.5)	9.01 ± 0.25 (9.53)	25
PBDB-TF: ITIC-C9	-	1.02 ± 0.01 (1.03)	13.9 ± 0.10 (14.0)	13.9 ± 0.10 (14.0)	58.2 ± 0.8 (59.0)	8.30 ± 0.11 (8.43)	6
	160	0.99 ± 0.01 (0.99)	13.4 ± 1.1 (15.7)	14.4 ± 0.2 (14.7)	66.6 ± 1.4 (66.3)	9.53 ± 0.29 (10.24)	26
	190	0.97 ± 0.01 (0.97)	12.8 ± 0.1 (12.8)	12.8 ± 0.1 (12.8)	65.7 ± 0.9 (66.2)	8.16 ± 0.11 (8.24)	4

Photovoltaic parameters are reported as averages ± one standard deviation. Numbers in parenthesis are for the champion cells. Thermal annealing is performed for 10 min at the listed temperature. Devices with no listed annealing temperature were not annealed.

[a] Current measured from integration of external quantum efficiency (EQE) spectra.

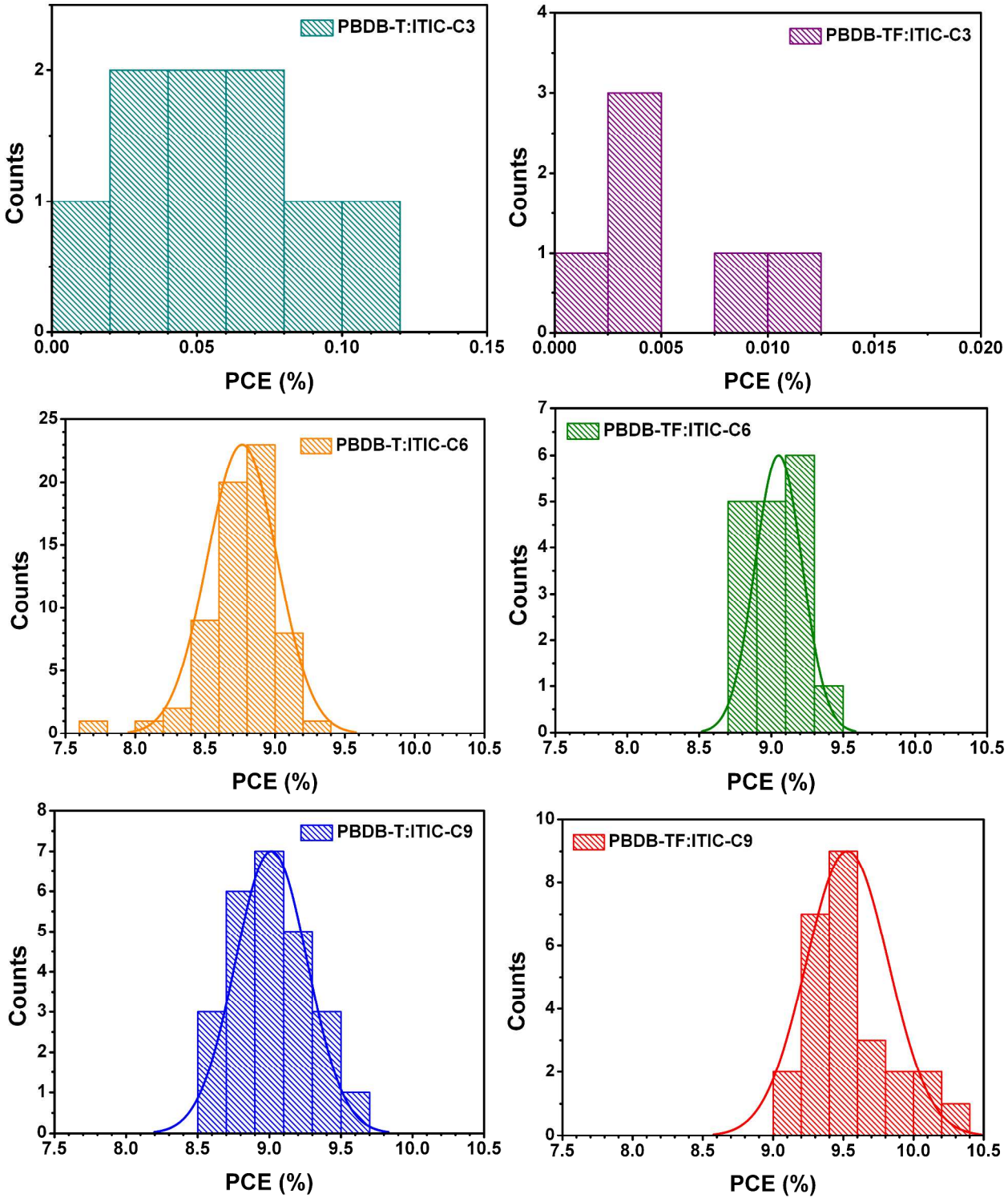

Figure S6. Histograms of power conversion efficiency (PCE) data for donor polymer:**ITIC-CX** solar cell devices subjected to thermal annealing at 160 °C.

ANOVATwoWay (8/15/2017 11:53:55)

Notes

Input Data

ANOVA

Overall ANOVA

	DF	Sum of Squares	Mean Square	F Value	P Value
ITIC-CX	1	3.45823	3.45823	54.99343	1.4252E-11
Donor Polymer	1	4.20418	4.20418	66.85569	2.3781E-13
Interaction	1	0.34139	0.34139	5.42884	0.02136
Model	3	10.91164	3.63721	57.83964	0
Error	129	8.1121	0.06288	--	--
Corrected Total	132	19.02374	--	--	--

At the 0.05 level, the population means of **ITIC-CX** are **significantly** different.
At the 0.05 level, the population means of **Donor Polymer** are **significantly** different.
At the 0.05 level, the interaction between **ITIC-CX** and **Donor Polymer** is **significant**.

Means Comparisons

Tukey Test

ITIC-CX

	MeanDiff	SEM	q Value	Prob	Alpha	Sig	LCL	UCL
ITIC-C9 ITIC-C6	0.45219	0.04472	14.29969	2.10166E-8	0.05	1	0.36371	0.54067

Donor Polymer

	MeanDiff	SEM	q Value	Prob	Alpha	Sig	LCL	UCL
PBDB-T PBDB-TF	-0.50591	0.04649	15.39036	2.10166E-8	0.05	1	-0.59789	-0.41393

Sig equals 1 indicates that the means difference is significant at the 0.05 level.
Sig equals 0 indicates that the means difference is not significant at the 0.05 level.

Figure S7. Two way ANOVA analysis indicating that the mean PCE of **ITIC-C9** devices is significantly different than that of **ITIC-C6** devices and that the mean PCE of **PBDB-TF** devices is significantly different than that of **PBDB-T** devices. Only PCE data from annealed (160 °C) devices are considered.

10. Atomic Force Microscopy (AFM) Characterization

AFM measurements were taken on a Dimension Icon scanning probe microscope (Bruker) in tapping mode. The blend thin films used were prepared in the same way as the optimized photovoltaic devices and spun cast on Si/ZnO substrates and then annealed at 160 °C for 10 min. (Section 9 in SI). Pristine films were spun cast on Si/ZnO substrates from chlorobenzene:1,8-diiodooctane (99:1 v:v) solutions (10 mg/mL concentration).

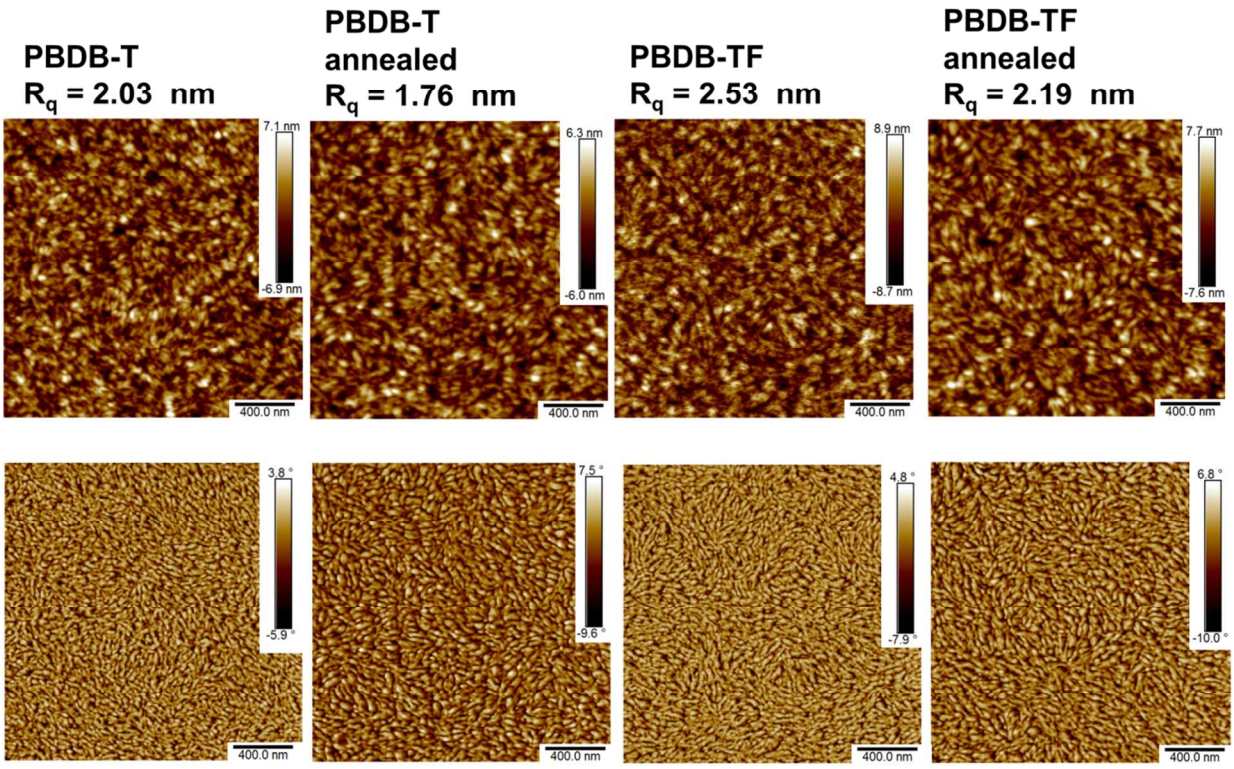

Figure S8. AFM topographical images (top) and phase images (bottom) of pristine donor polymer films.

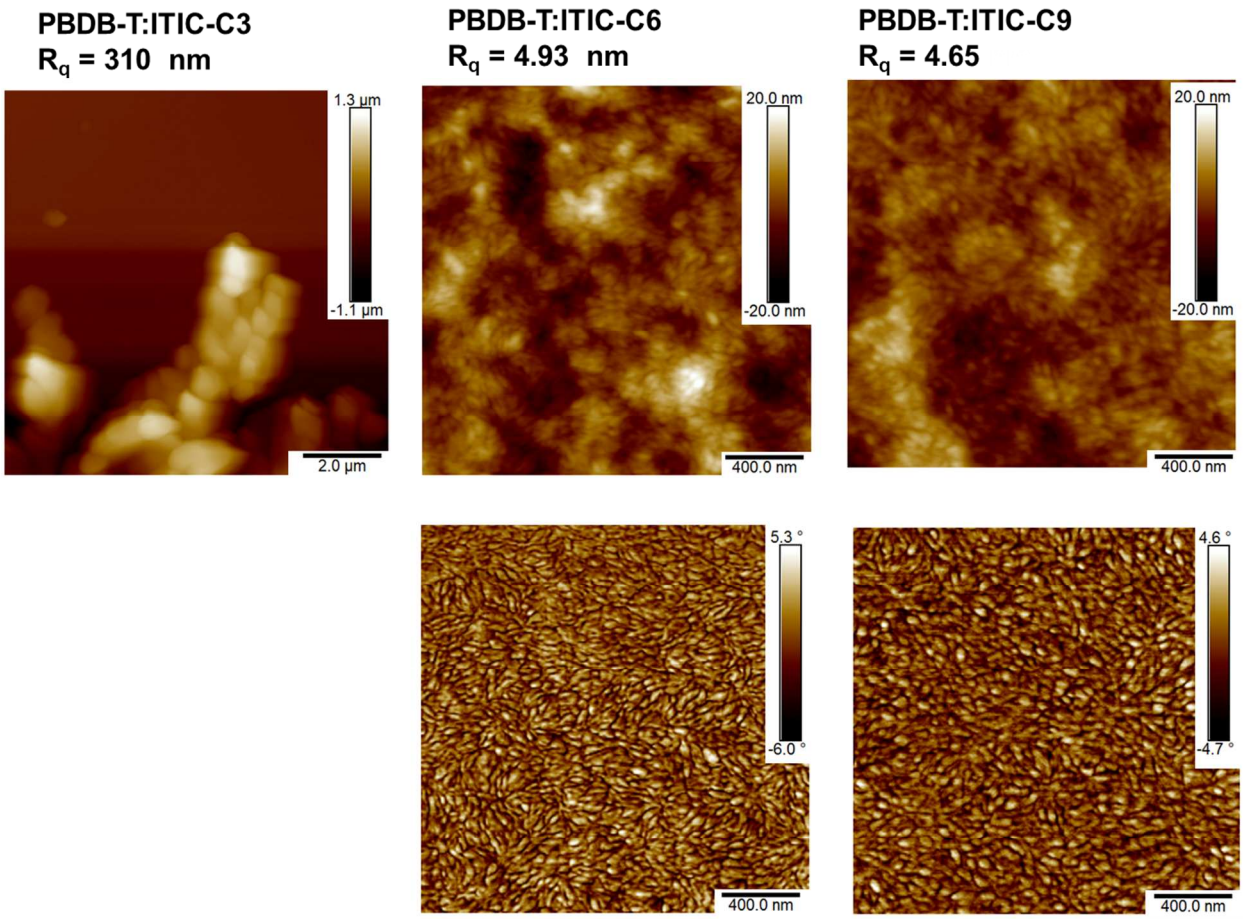

Figure S9. AFM topographical images (top) and phase images (bottom) of **PBDB-T:ITIC-CX** annealed films.

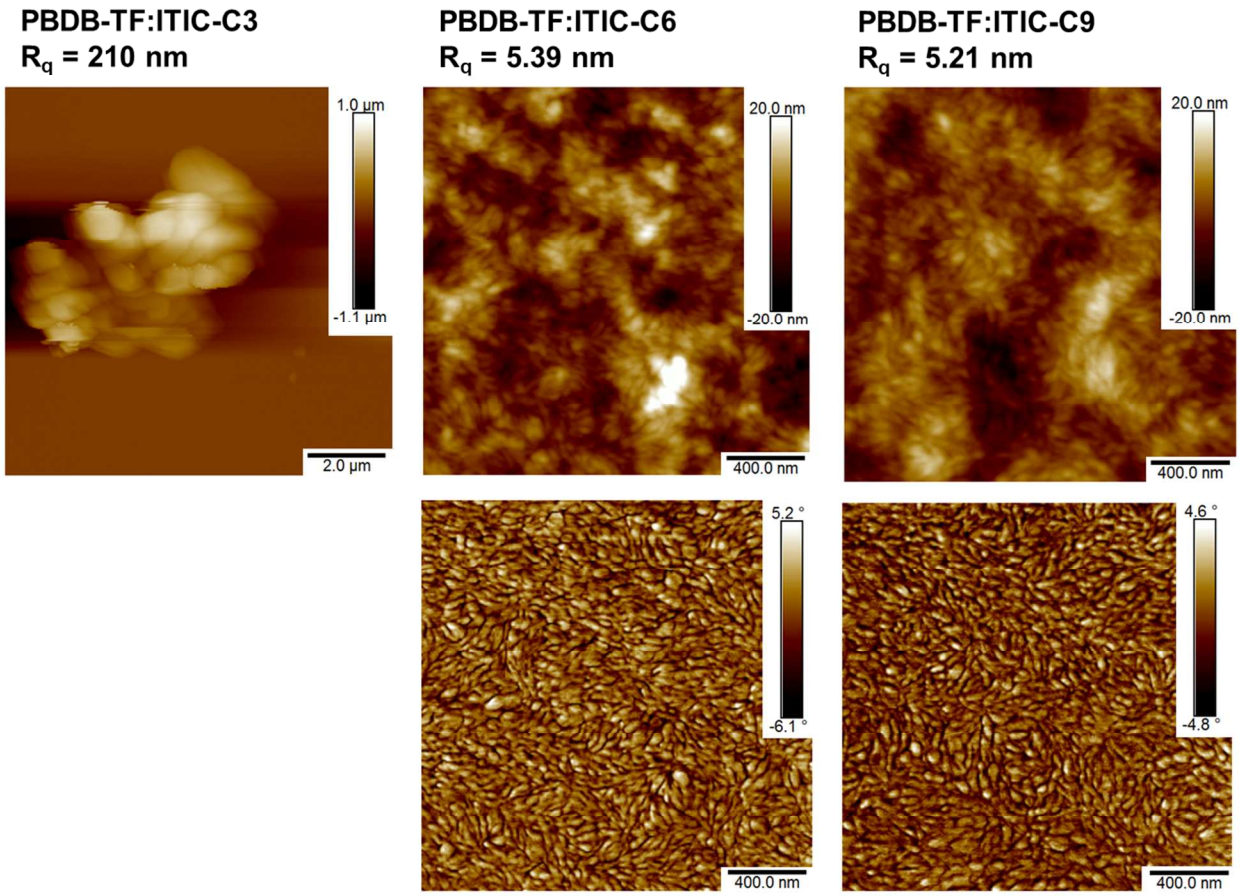

Figure S10. AFM topographical images (top) and phase images (bottom) of **PBDB-TF:ITIC-CX** annealed films.

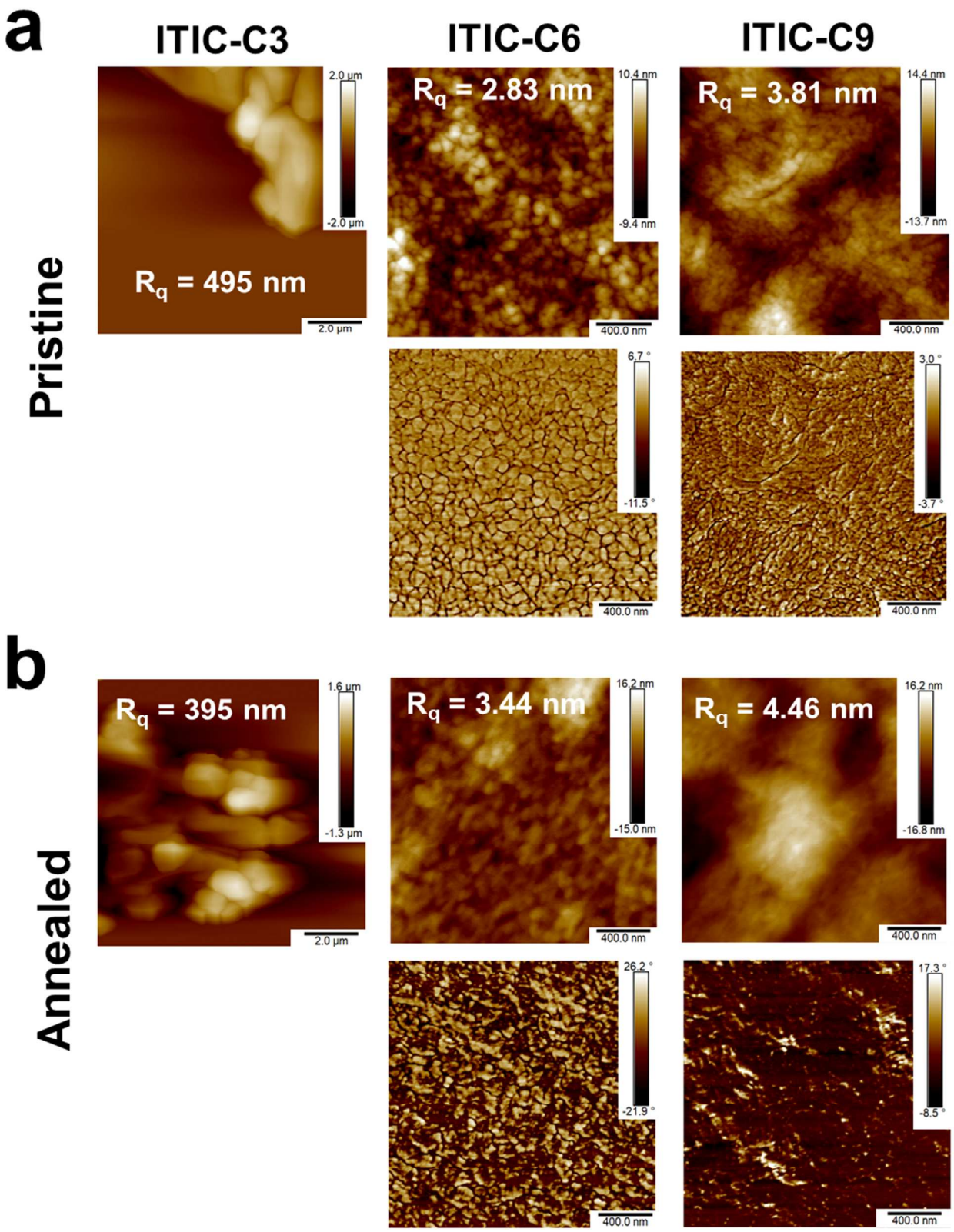

Figure S11. (a) AFM topographical images (top) and phase images (bottom) of **ITIC-CX** pristine films. (b) AFM topographical images (top) and phase images (bottom) of **ITIC-CX** annealed films.

11. X-Ray Diffraction (XRD) Measurements

The donor polymer:**ITIC-CX** blend films were prepared using the optimized device conditions on Si/ZnO substrates and then annealed at 160 °C for 10 min. Pristine films were spun cast on Si/ZnO substrates from chlorobenzene:1,8-diiodooctane (99:1 v:v) solutions (10 mg/mL concentration). Thin films were analyzed using wide-angle X-ray scattering (WAXS) on a Rigaku Smartlab diffractometer using standard out-of-plane 2θ technique (thin-film XRD), with monochromated CuK_α radiation (λ = 1.541 Å). Diffraction peaks were fitted with Bragg's equation $n\lambda = 2d\sin\theta$ to obtain lamellar (d_{100}) and π-π (d_{010}) stacking distances, respectively.

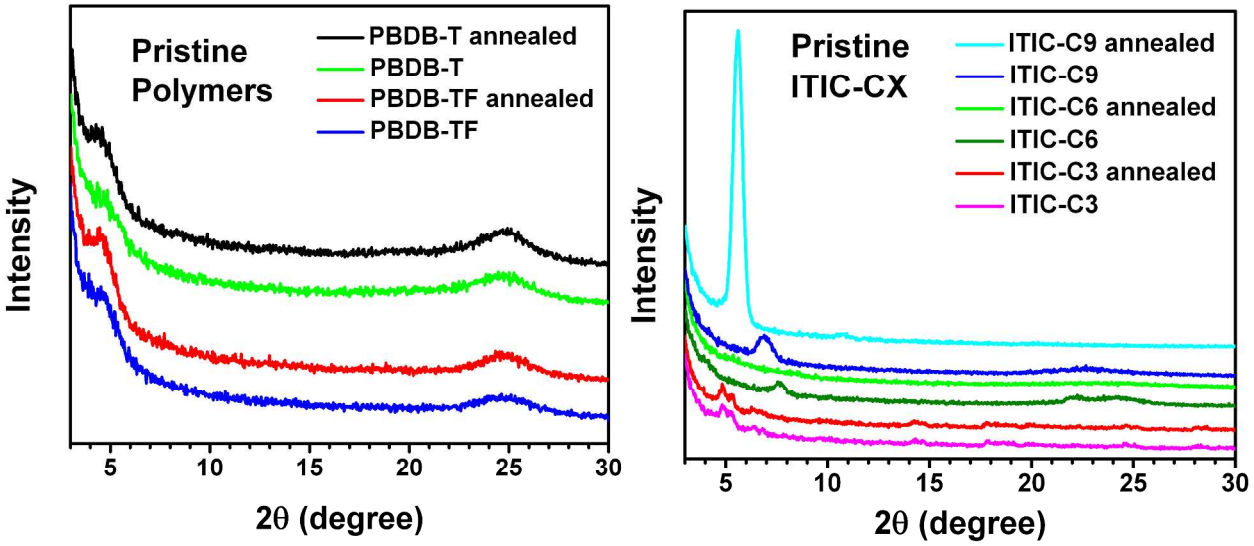

Figure S12. 2θ XRD scattering patterns from donor polymer pristine films (left) and **ITIC-CX** pristine films (right). Data has been stacked for clarity.

The lamellar reflection peak in **ITIC-C9** pristine annealed film was fit to the Scherrer equation to approximate the grain size τ (eq. 1)[6]:

$$\tau = \frac{K\lambda}{\beta \cos\theta} \quad (1)$$

where $K = 0.9$, $\lambda = 1.541$ Å, $\beta = 9.36 \times 10^{-3}$ rad, and $\theta = 4.88 \times 10^{-2}$ rad. Thus, $\tau = 14.9$ nm.

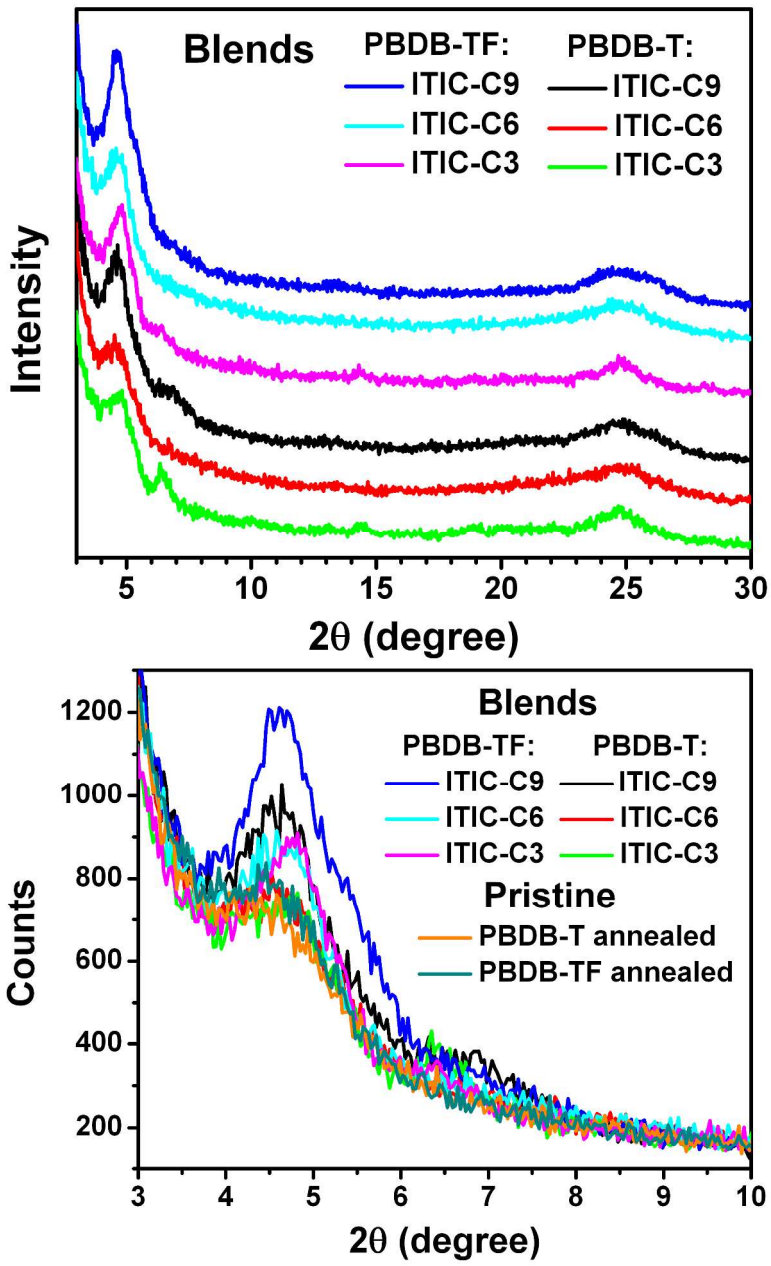

Figure S13. 2θ XRD scattering patterns from donor polymer:**ITIC-CX** blend films. (top) Data has been stacked for clarity. (bottom) Selected region of 2*θ* XRD scattering patterns from donor polymer:**ITIC-CX** blend films and pristine donor polymers.

Table S6. XRD data for donor polymers, **ITIC-CX**, and blends.

Film		2θ <100> (°)	Lamellar distance out-of-plane d_{100} (Å)	2θ <010> (°)	π–π distance out-of-plane d_{010} (Å)
ITIC-C9	pristine	6.848	12.90	22.50	3.95
	annealed	5.587	15.81	–	–
	PBDB-T	4.546	19.43	24.62	3.61
	PBDB-TF	4.621	19.11	24.80	3.59
ITIC-C6	pristine	7.599	11.63	22.24	4.00
				24.08	3.69
	annealed	–	–	22.24	4.00
	PBDB-T	4.441	19.89	24.71	3.60
	PBDB-TF	4.589	19.25	24.57	3.62
ITIC-C3	pristine	4.902	18.02		
	annealed	4.835	18.27		
	PBDB-T	4.651	18.99	24.64	3.61
		6.410	13.78		
	PBDB-TF	4.742	18.62	24.74	3.60
PBDB-T	pristine	4.352	20.29	24.43	3.64
	annealed	4.240	20.83	24.63	3.61
PBDB-TF	pristine	4.471	19.75	24.51	3.63
	annealed	4.412	20.02	24.63	3.61

12. Grazing Incidence Wide-Angle X-Ray Scattering (GIWAXS) Measurements

The **ITIC-CX** pristine films were spun cast on Si/ZnO substrates from chlorobenzene:1,8-diiodooctane (99:1 v:v) solutions (10 mg/mL concentration) and thermal annealing was conducted at 160 °C for 10 min. GIWAXS measurements were performed at beamline 8ID-E at the Advanced Photon Source at Argonne National Laboratory. The samples were irradiated at incidence angles from 0.130° to 0.140° in vacuum at 10.915 keV for two summed exposures of 2.5 s each. Signals were collected with a Pilatus 1M detector located at a distance of 228.165 mm from the samples.

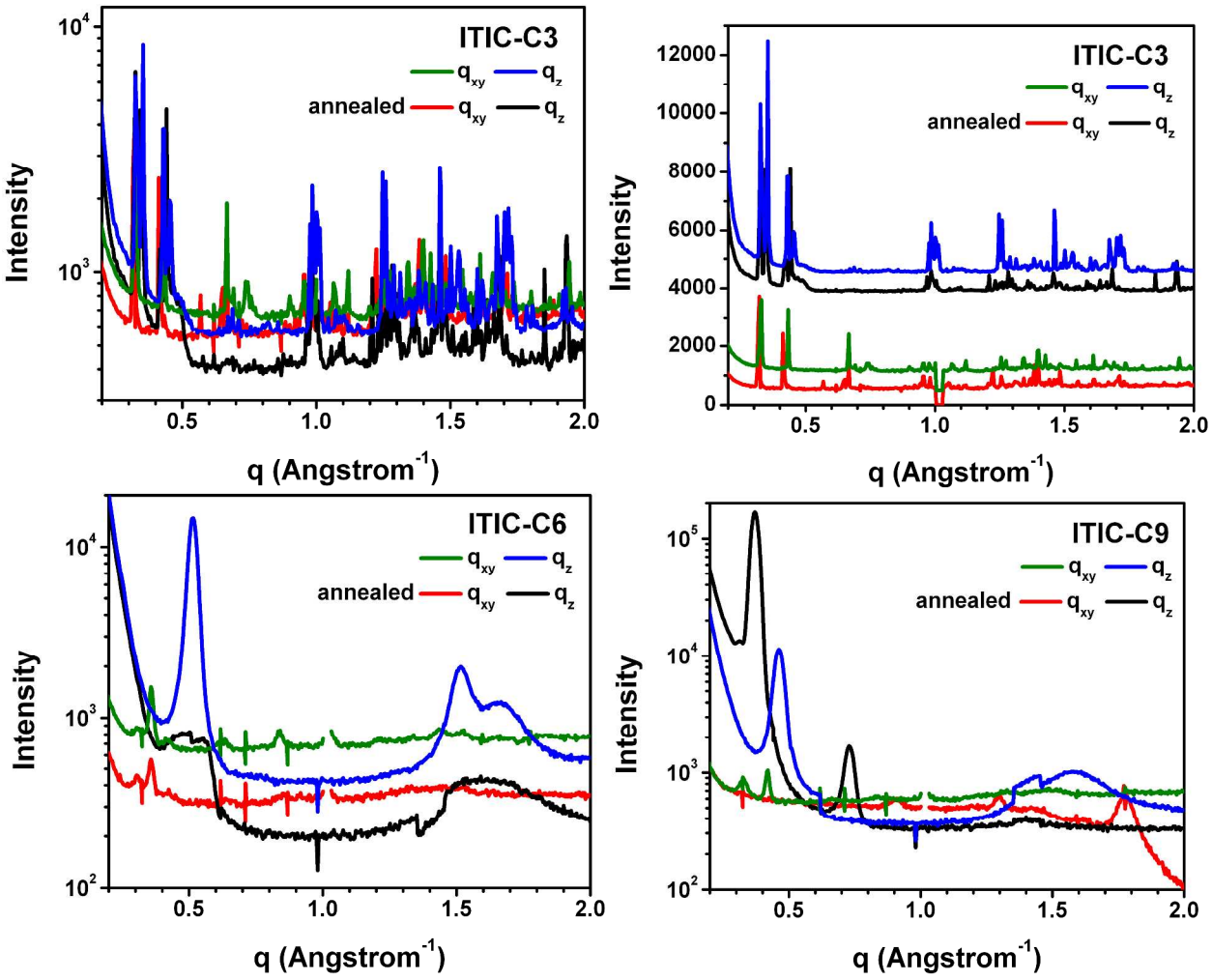

Figure S14. GIWAXS line cuts of the **ITIC-CX** pristine films showing in-plane (q_{xy}) and out-of-plane (q_z) crystalline peaks and the effects of thermal annealing. **ITIC-C3** data (right) is stacked for clarity and plotted on a linear scale.

13. SCLC Mobility Measurements

Hole-only diodes were fabricated using the structure: ITO/PEDOT:PSS/active layer/MoO_3 (9 nm) /Au (150 nm). Electron-only diodes were fabricated using the structure: ITO/ZnO/active layer/LiF (1 nm) /Al (100 nm). The top contact was the injecting electrode in both cases. Electron-only diodes were measured in vacuum (~10^{-6} Torr) and hole-only diodes were measured in air. The semiconducting polymer:ITIC-CX layers were prepared in the same way as for the optimized photovoltaic devices (Section 9 in SI). Pristine films were spun cast from chlorobenzene:1,8-diiodooctane (99:1 v:v) solutions (10 mg/mL concentration) and annealed at 160 °C for 10 min.. The SCLC mobility was derived by fitting the *J–V* curve in the space charge limited regime following eq. 2.[7]

$$J = \frac{9}{8}\varepsilon_s \frac{V_{eff}^2}{d^3}\mu_0 exp\left(\gamma\sqrt{\frac{V_{eff}}{d}}\right) \quad \textbf{(2)}$$

Here, J is the current density, the parameter γ controls the field dependence of the current, μ_0 is the zero-field mobility, ε_s and d are the semiconductor permittivity (taken as $3\varepsilon_0$) and diode thickness (measured by Veeco Dektak 8 profilometer), respectively. The V_{eff} was calculated by correcting the applied voltage for the series resistance of the ITO (20 Ω/) and the built-in voltage (V_{bi}) of the device: $V_{eff} = V_{appl} - V_{bi} - V_{RS}$, where $V_{RS} = JAR_{series}$. For hole-only diodes V_{bi} = 0.1 V, and for electron-only devices V_{bi} = 0.7 V. Device dimensions were 200 μm × 200 μm with an area (A) of 4 × 10^{-8} m^2. Mobilities are reported as averages taken over 4 or more separate devices ± one standard deviation (1σ).

Table S7. SCLC electron and hole mobilities.

Film	$\mu_h \times 10^4$ ($cm^2V^{-1}s^{-1}$)	$\mu_e \times 10^6$ ($cm^2V^{-1}s^{-1}$)
PBDB-T	3.9 ± 0.9	-
PBDB-TF	9.8 ± 1.5	-
ITIC-C6	-	0.14 ± 0.13
ITIC-C9	-	2.1 ± 1.1
PBDB-T : ITIC-C6	8 ± 3	5.4 ± 0.6
PBDB-T : ITIC-C9	8 ± 3	30 ± 20
PBDB-TF : ITIC-C6	8 ± 3	6 ± 3
PBDB-TF : ITIC-C9	17 ± 4	16 ± 11

14. References

1. Xu, Y.-X.; Chueh, C.-C.; Yip, H.-L.; Ding, F.-Z.; Li, Y.-X.; Li, C.-Z.; Li, X.; Chen, W.-C.; Jen, A. K.-Y. *Adv. Mater.* **2012**, *24*, 6356-6361.
2. Bello, K. A.; Cheng, L.; Griffiths, J. *J. Chem. Soc., Perkin Trans. 2*, **1987**, *0*, 815-818.
3. Zhang, M.; Guo, X.; Zhang, S.; Hou, J. *Adv. Mater.* **2014**, *26*, 1118-1123.
4. Qian, D.; Ye, L.; Zhang, M.; Liang, Y.; Li, L.; Huang, Y.; Guo, X.; Zhang, S.; Tan, Z.; Hou, J. *Macromolecules* **2012**, *45*, 9611-9617.
5. Henson, Z. B.; Welch, G. C.; van der Poll, T.; Bazan, G. C. *J. Am. Chem. Soc*. **2012**, *134*, 3766-3779.
6. Smilgies, D.-M. *J. Appl. Crystallogr*. **2009**, *42*, 1030-1034.
7. Murgatroyd, P. N. *J. Phys. D: Appl. Phys.* **1970**, *3*, 151-156.